Research Article Open Access

Journal of Modern Classical Physics & Quantum Neuroscience

ISSN: 3068-4196

DOI: doi.org/10.63721/26JPQN0179

New Interpretation of Quantum Mechanics with Time-retrograde Waves

Yoshiya Higuchi

Ibaraki, Japan

Citation: *Yoshiya Higuchi (2026) New Interpretation of Quantum Mechanics with Time-retrograde Waves. J.of Mod Phy & Quant Neuroscience 2(5), 1-44. WMJ/JPQN-179*

Abstract

This study interprets four major mysteries related to observation in quantum mechanics. These are based on a new interpretation of the energy–time uncertainty relation, which yields time retrogression and suggests that a quantum state's time evolution may fluctuate if measurement fixes its energy. The resulting time-reversed state is represented by a bra vector. The time reversed bra vector and the time-evolving ket vector interact along the time axis to generate a time-invariant bra–ket state, indicating state determination. The first topic is why observation selects one state from a superposition. Among all time-reversed states, the state with the least energy dispersion reaches farthest into the past, establishing that state while the others disappear. The existence of a single state in the farthest past explains quantum state contraction induced by observation. The second topic is the spatial contraction of the wave packet upon observation. In QFT, the wave functions forming the wave packet arise from vacuum energy fluctuations which disappear through the inner product in the bra–ket state. Consequently, external vacuum energy exerts a compressive force that contracts the wave packet. This mechanism explains both state selection and spatial contraction upon observation. The third topic is long-range correlation without transmission time in quantum entanglement. This study explains that photon states go back into the past and are determined there, accounting for the simultaneous correlation between distant photons. The fourth topic is the origin of randomness in measurement outcomes. This study interprets randomness in energy dispersion as arising from phase differences between measuring-device states. Thus, the state is determined probabilistically yet deterministically through measurement. These interpretations reinforce local-reality and restore determinism in quantum mechanics.

***Corresponding author:** Yoshiya Higuchi, Tokai 3-2-46-204 Tokai Vil. Ibaraki, 3191117, Japan.

Submitted: 20.06.2026 **Accepted**: 26.06.2026 **Published:** 15.09.2026

Introduction

Quantum state contraction after observation remains a long-standing mystery in quantum mechanics. Although the von Neumann projection operator [1] mathematically accounts for this phenomenon by extracting a single state from a superposition of state vectors obtained through measurement, the underlying physical principles remain elusive. To bridge this gap in understanding, the present study sought to explain quantum state contraction using quantum time reversal.

Since the formulation of quantum mechanics, the nature of the wave function has been extensively debated [2]. If the wave function faithfully represents the behavior of elementary particles such as electrons, clarifying its nature becomes identical to understanding the ontological status of the particles themselves. In quantum field theory (QFT), elementary particles are interpreted as excited states of the vacuum, suggesting that the wave function in quantum mechanics may manifest vacuum-field energy. This view further motivates a reexamination of long-standing problems such as wave packet collapse upon measurement, which remains a central topic of debate in quantum mechanics [3].

Similarly, long-range correlation without transmission time between two entangled quanta is difficult to interpret because it violates the requirements of the theory of relativity. This study also attempts to explain this phenomenon through quantum time reversal.

More broadly, quantum mechanics has transformed the Newtonian worldview by revealing that measurement probabilistically determines quantum mechanical states and that this process is inherently nondeterministic. Thus, quantum mechanics rejects naive realism, which assumes that the state of a physical system is defined before measurement. In parallel, it rejects a deterministic worldview wherein a system's temporal evolution entirely determines its future state.
This study interprets these problems in quantum mechanics as involving quantum states that propagate forward and backward in time.

1. Interpretation of the Quantum State Contraction Using Time-Reversed Waves [4]

Early notion of retro-causality in quantum optics was introduced by de broglie [5]. Costa de Beauregard also studied the interpretation of quantum mechanics by time symmetry [6].

To date, several theories have been proposed to elucidate quantum-mechanical principles in terms of forward and backward propagation in time. These theories include the transactional interpretation of quantum mechanics (TI) by Cramer et al. , the two-state vector formalism (TSVF) of Aharonov et al, and the absorber theory (AT) proposed by Pegg [7-9].

In the TI framework, anterograde and retrograde waves are exchanged between the observed wave emitter and absorber. During this exchange, waves lying outside the emitter and absorber vanish owing to the superposition of opposite phases, while in-phase waves lying between them interfere constructively. This constructive interference leads to the contraction of states. However, in this framework, the mechanism triggering the propagation of the confirmation wave in the negative time direction upon the arrival of the offer wave at the absorber remains unknown.

The TI theory is rooted in the framework of the Wheeler–Feynman radiation theory, which involves the two solutions of the classical electromagnetism propagation equation: one representing forward propagation and the other describing backward propagation in time [10]. Notably, if this concept is to be extended to general quanta, the quanta must possess two solutions, one directed forward and the other directed backward in time. However, since the Schrödinger equation, which governs non-relativistic quantum mechanics, is a first-order differential equation with respect to time, it has only one type of solution in the time domain. For the acquisition of dual-time-directed solutions in general quantum mechanics, considerations based on relativistic quantum mechanics are necessary [12].

In relativistic quantum mechanics, both the Klein–Gordon equation, describing Bose particles, and the Dirac equation, modelling Fermi particles, come into play. While the former, being a second-order differential equation with respect to time, permits the simultaneous existence of solutions directed forward and backward in time, the latter, being a first-order differential equation with respect to time, has only one type of solution in the time domain.

Nonetheless, the Dirac equation has four simultaneous solutions associated with charge and spin, and its antiparticle solution could be considered to describe time reversal. However, in this framework, overlapping particle and antiparticle waves traveling backward in time do not reinforce each other but rather annihilate each other.

Cramer's transactional interpretation of quantum mechanics posits that confirmation waves traveling towards the past, similar to electromagnetic waves, are not always pre-existing waves, but are rather generated upon receipt of offer waves propagating forward in time. However, the mechanism underlying the formation of these incoming confirmation waves remains unknown.

Notably, the TSVF uses both past and future states to ascertain the current state, and it determines the probability of acquiring a weak measurement that is incapable of inducing system decoherence. However, the theory does not elaborate on the process through which the state vector is influenced across the period extending from the future to the past.

The AT of Pegg shares similarities with the interpretations of Aspect et al.'s experiment [13] provided in a previous study [14]. The theory represents an application instance of the Wheeler–Feynman radiation theory, and it considers the consistent presence of advanced photon waves traveling backward in time. However, the applicability of this theory is restricted to photons. Notably, Einstein–Podolsky–Rosen correlations similar to those observed in Aspect et al.'s experiment have been confirmed in experiments involving general quanta such as protons [11]. Consequently, relying solely on the photon theory, which proposes the existence of a retrograde wave solution, is inadequate.

Against this background, the current study posits that time retrogression is a property permitted by the energy-time uncertainty relation, and it considers that if the energy of a system is determined, the system's temporal evolution may exhibit fluctuations, enabling time travel into the past.

1.1 The Uncertainty Relation Between Energy and Time

The uncertainty relation between energy and time — $\Delta E \Delta t \geq \frac{\hbar}{2}$ — is derived from the uncertainty relation between position and momentum ($\Delta q \Delta p \geq \frac{\hbar}{2}$). Thus, the former relation is not considered to represent a fundamental principle.

Furthermore, this relation does not imply the existence of the following canonical conjugate relation between time and energy: $[E, t] = i\hbar$. Notably, Pauli refuted this canonical conjugation [15], and this implies that time functions as a parameter and not as an observable. Consequently, determining the eigenvalue of time becomes impossible. In particular, energy cannot be constrained to negative values.

Various interpretations have been provided for the uncertainty of energy and time [16]. The widely accepted interpretation of the energy-time uncertainty relation is that involving the time scale of state change, proposed by Mandelstam and Tamm [17].

However, Arai showed that the following canonical commutation relation exists between a symmetric operator T and a self-adjoint operator H [18]:

$$[T, H] = i. \tag{1}$$

Let H and T are on a complex Hilbert space $\mathcal{H}$, $\sigma(T)$ be the spectrum of T, and $\mathbb{C}$ is the set of complex numbers. Then, the following statements hold.

(i) If H is bounded below, then $\sigma(T)$ is either $\mathbb{C}$ or $\{z \in \mathbb{C} \mid \mathrm{Im}z \geq 0\}$.
(ii) If H is bounded above, then $\sigma(T)$ is either $\mathbb{C}$ or $\{z \in \mathbb{C} \mid \mathrm{Im}z \leq 0\}$.
(iii) If H is bounded, then $\sigma(T)$ is either $\mathbb{C}$.

Here, owing to the positive definiteness of the energy, following Pauli [15], we adopt condition (i). The time that we are aware of in this world is a real number. Hence, the spectrum contains the real axis of time.

The energy-time uncertainty relation $\Delta E \Delta t \geq \frac{\hbar}{2}$ suggests that if $\Delta t < 0$, then $\Delta E < 0$. Furthermore, fluctuations in ΔE around $E_0 = 0$ would lead to situations with $E < 0$ (Figure 1(a)).

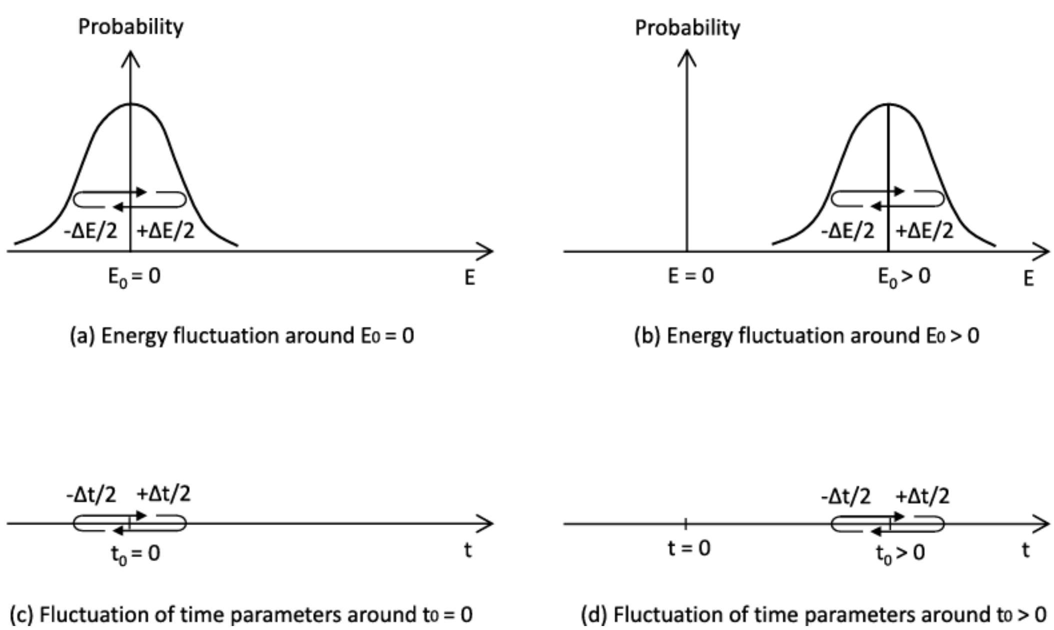

Figure 1: Fluctuations of energy and time parameters

However, when Δt and ΔE are considered as fluctuation widths, that is, $\Delta t > 0$ and $\Delta E > 0$, and fluctuations occur around E_0 such that $E_0 > \frac{\Delta E}{2} > 0$, the resulting energy E, including the fluctuations, can be expressed as $E = E_0 \pm \frac{\Delta E}{2} > 0$. Clearly, this expression yields positive E values (Figure 1(b)).

In the context of time, the sign lacks intrinsic significance, except for the assumption of a positive value for the current time. From this perspective, $t_0 = 0$ serves as a relative coordinate on the time axis (Figure 1(c)). Notably, when time fluctuates around the centre, we hypothesise the possibility of a very small retrogression of time around $t_0 > 0$ (Figure 1(d)).

Thus, the energy-time uncertainty relation permits the reversal of time without necessitating negative energy values. According to the uncertainty relation $\Delta E \Delta t \geq \frac{\hbar}{2}$, the determination of the energy through measurement leads to a corresponding fluctuation in time, denoted by Δt, implying that the time can shift in the negative direction by approximately half of this fluctuation. For such a negative fluctuation of $\frac{\Delta t}{2}$, the quantum state undergoes time reversal.

1.2 Time Reversal and Physical State Change by Observation

In quantum mechanics, the Schrödinger equation is an equation of motion for the state vector:

$$i\hbar \frac{\partial}{\partial t} |\psi(\mathbf{x}, t)\rangle = \hat{H} |\psi(\mathbf{x}, t)\rangle. \tag{2}$$

Under time reversal, the time derivative operator transforms as

$$\frac{\partial}{\partial t} \to \frac{\partial}{\partial(-t)} = -\frac{\partial}{\partial t}. \tag{3}$$

The complex conjugate of (2) is a time-reversed form of (2):

$$i\hbar \frac{\partial}{\partial t} \langle\psi(\mathbf{x}, t)| = \langle\psi(\mathbf{x}, t)| \hat{H}. \tag{4}$$

Where

$$|\psi(\mathbf{x}, t)\rangle^\dagger = \langle\psi(\mathbf{x}, t)|. \tag{5}$$

Furthermore, we assume

$$\hat{H}^\dagger = \hat{H}. \tag{6}$$

Thus, time reversal is modeled by an antiunitary transformation, under which the state vector becomes the complex conjugate of the original [19]. Here, if the original state vector is denoted by the ket vector $|\psi\rangle$, its complex conjugate is represented by the bra vector $\langle\psi|$.

The rationale behind the simultaneous requirement of the complex conjugation and the transposition of the state vector is as follows: First, within the realm of this study, the vector inner product is not merely a mathematical operation but regarded as a physical process. Furthermore, the generation of the bra vector essential for this inner product operation necessitates time reversal.

Generally, the energy of a quantum state $|\psi(t)\rangle$ is determined by the individual contributions of its eigenstates $|\psi_i(t)\rangle$. According to the uncertainty relation between time and energy, certaining a energy for the state $|\psi_i(t)\rangle$ introduces a fluctuation Δt in the time parameter, allowing for the conceptual possibility of the backward propagation of time, thus generating a time-reversed wave $\langle\psi_i(t)|$.

Notably, the time evolution of state $|\psi_i(t)\rangle$ can be modeled as a unitary transformation:

$$|\psi_i(t)\rangle = e^{-\frac{i\hat{H}t}{\hbar}}|\psi_i\rangle. \tag{7}$$

On the other hand, the time evolution of the time-reversed state $\langle\psi_i(t)|$ can be modeled as an antiunitary transformation:

$$\langle\psi_i(t)| = \langle\psi_i|e^{\frac{i\hat{H}t}{\hbar}}. \tag{8}$$

When $\langle\psi_i(t)|$ and $|\psi_i(t)\rangle$ combine along the time axis, they generate $\langle\psi_i(t)|\psi_i(t)\rangle$, which can be expressed as follows:

$$\langle\psi_i(t)|\psi_i(t)\rangle = \langle\psi_i|e^{\frac{i\hat{H}t}{\hbar}}e^{-\frac{i\hat{H}t}{\hbar}}|\psi_i\rangle = \langle\psi_i|\psi_i\rangle. \tag{9}$$

Thus, a time-invariant state results from combining of the states. This principle can also be used to ascertain superposed state $|\psi(t)\rangle$ that has not been determined on the time axis:

$$\langle\psi_i(t)|\psi(t)\rangle = \langle\psi_i|e^{\frac{i\hat{H}t}{\hbar}}e^{-\frac{i\hat{H}t}{\hbar}}|\psi\rangle = \langle\psi_i|\psi\rangle = \langle\psi_i|\psi_i\rangle. \tag{10}$$

Thus, the established bra state $\langle\psi_i(t)|$ can be used to determine the ket superposition state $|\psi(t)\rangle$.

This study calls the state of equation (9) the ‘bra-ket state’. This state becomes a static state without time variation because the time-evolving operator is cancelled by the operator that evolves in the opposite direction, as shown in equation (9). Also, by taking the inner product of the bra state and the ket state, the quantity of this bra-ket state becomes the C number. Each state in the superposition has a complex coefficient like as $a_i|\psi_i\rangle$. In this case, the bracket state is $|a_i|^2\langle\psi_i|\psi_i\rangle = |a_i|^2$, which corresponds to the probability of obtaining this by measurement as in the Born’s interpretation.

These equations appear to simply express the stationary and orthonormal nature of the energy eigenstates that we are familiar with. However, this study argues that these are not just mathematical expressions of the quantum mechanical energy eigenstates that have been introduced so far, but that these processes of determining the states by such time-reversed bra vectors occur as physical phenomena.

This type of time reversal occurs when the quantum system interacts with some external system, such as a measuring device, as will be shown in the next section. At this time, energy fluctuations occur in the quantum system, and the time parameter fluctuates due to the uncertain relationship between energy and time. This fluctuation in the time parameter can occur in either the positive or negative direction, and a time parameter that fluctuates in the negative direction causes time reversal in the quantum system.

In this case, if an interaction with an external system occurs at $t = t_0$ and the fluctuation of the time parameters begins, the boundary condition for the time-reversed wave is $\langle\psi_i(t_0)| = \langle\psi_i|e^{\frac{i\hat{H}t_0}{\hbar}}$, and the boundary condition for the time-progressive wave is $|\psi_i(t_0)\rangle = e^{-\frac{i\hat{H}t_0}{\hbar}}|\psi_i\rangle$.

1.3 Quantum State Contraction due to Time-Retrograde Waves

By identifying the state generated by the time-reversed vector through observation, we can describe the mechanism of quantum state contraction due to the observation as follows. Let us suppose that before observation, the quantum state is in the superposition state

$$|\psi\rangle = a_1|\psi_1\rangle + a_2|\psi_2\rangle + \cdots + a_m|\psi_m\rangle + \cdots. \tag{11}$$

When we attempt to ascertain this state through observation, each component state $a_1|\psi_1\rangle, a_2|\psi_2\rangle, \cdots, a_m|\psi_m\rangle, \cdots$ begins to establish itself. This process reduces the energy fluctuation widths of the states, namely $\Delta E_1, \Delta E_2, \cdots, \Delta E_m, \cdots$. Ultimately, the state with the smallest energy fluctuation width is probabilistically determined.

Concurrently, the time fluctuation widths $\Delta t_1, \Delta t_2, \cdots, \Delta t_m, \cdots$ increase, in accordance with the energy-time uncertainty relation $\Delta t \geq \frac{\hbar}{2\Delta E}$. The state with the largest time fluctuation width is determined stochastically, according with the energy fluctuation width.

Depending on the time fluctuation width of each state vector, time reversal could occur, and the time-reversed vectors transform into the following bra vectors: $a_1{}^*\langle\psi_1|, a_2{}^*\langle\psi_2|, \cdots, a_m{}^*\langle\psi_m|, \cdots$. Among these bra vectors, the bra vector with the highest degree of energy certainty through measurement travels the farthest into the past. Figure 2 depicts this situation.

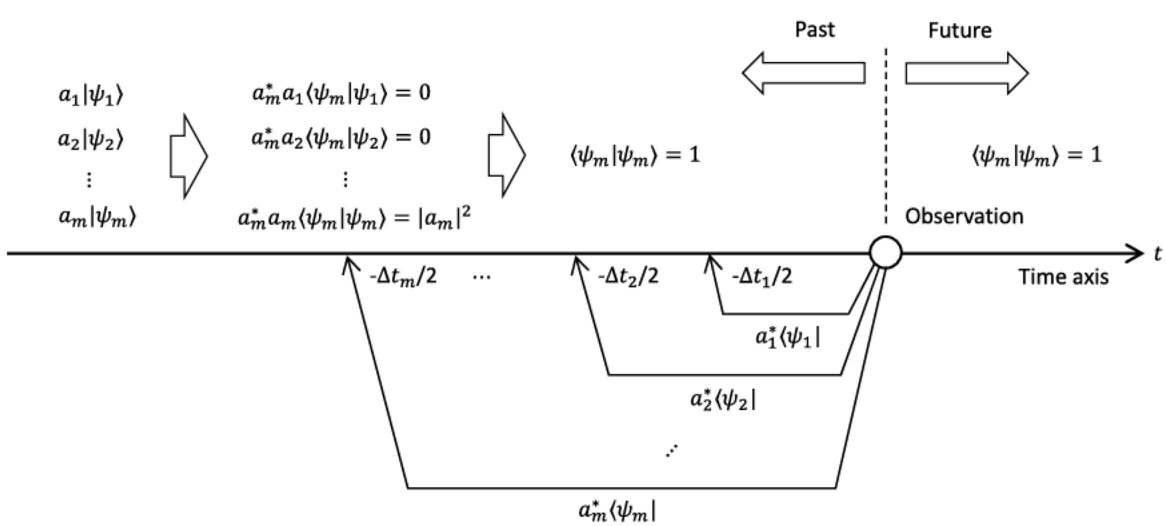

Figure 2: Contractions of quantum state by a state vector reaching the farthest past

In this scenario, the bra vector $a_m{}^*\langle\psi_m|$ reaches its farthest point in the past at $-\Delta t_m/2$. This bra vector $a_m{}^*\langle\psi_m|$ then interacts with states existing in the past, namely $a_1|\psi_1\rangle, a_2|\psi_2\rangle, \cdots, a_m|\psi_m\rangle, \cdots$, and the following relations hold.

$$a_m{}^*a_1\langle\psi_m|\psi_1\rangle = 0, \quad a_m{}^*a_2\langle\psi_m|\psi_2\rangle = 0, \quad \cdots, \quad a_m{}^*a_m\langle\psi_m|\psi_m\rangle = |a_m|^2, \quad \ldots \tag{12}$$

The above process can determine state $a_m|\psi_m\rangle$ with probability $|a_m|^2$, while the other states ($a_1|\psi_1\rangle, a_2|\psi_2\rangle, \cdots$) disappear. Although the bra vectors $a_1{}^*\langle\psi_1|, a_2{}^*\langle\psi_2|, \cdots$ reach $-\Delta t_1/2, -\Delta t_2/2, \cdots$, their corresponding ket vectors $a_1|\psi_1\rangle, a_2|\psi_2\rangle, \cdots$ have already disappeared. Therefore, the establishment of these states is prohibited.

This is the mechanism of quantum state contraction through observation.

The aforementioned time fluctuation also occurs in the future, as depicted in Figure 3. Specifically, under this time fluctuation, states $a_1|\psi_1\rangle, a_2|\psi_2\rangle, \cdots, a_m|\psi_m\rangle, \cdots$ traverse into the future from the observation point; however, these state vectors do not exist beyond the furthest future point located at $+\Delta t_m/2$.

Consequently, once the ‘present’ exceeds this fluctuation time, only the time-independent state $\langle\psi_m|\psi_m\rangle$ exists with a probability of one, according to Equation (10).

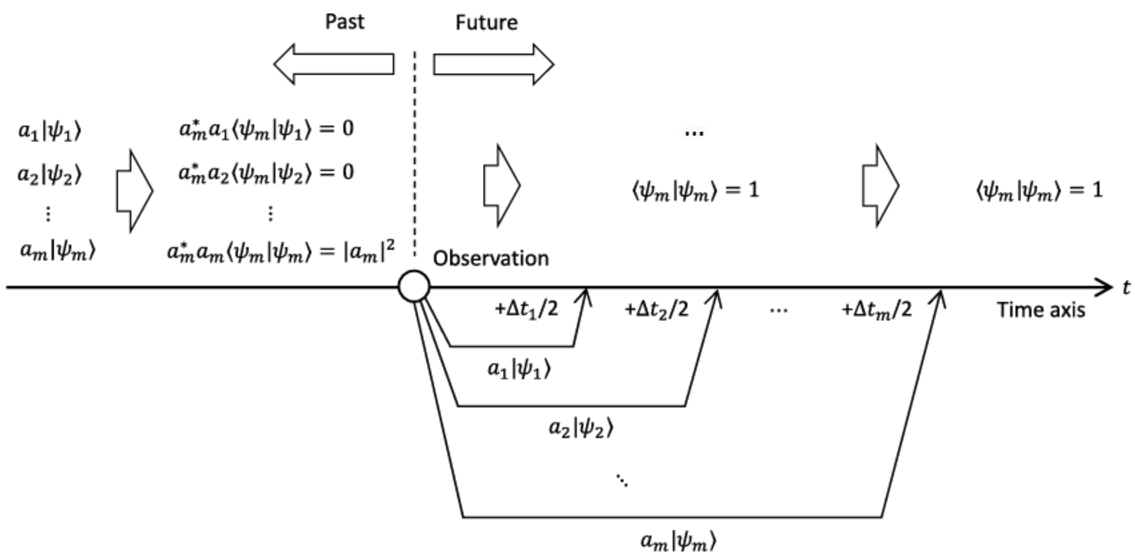

Figure 3: State vectors reaching the future

This completes the phenomenon of quantum state contraction. These processes, which have been described mathematically by von Neumann [1], occur as physical processes as outlined above.

Here, ‘measurement’ is considered to be a physical operation that limits the dispersion of energy states. The operation limiting the dispersion of momentum also limits the dispersion of energy states. Similarly, the operation limiting the dispersion of position also limits the dispersion of energy states.

When electron collides with a photographic plate to form a bright spot and identifies its final point reached [20], the electrons' energy is ultimately lost and defined to be zero. Hence, this collision process is an operation limiting the dispersion of energy states. Such limiting of the dispersion of energy states also occurs when photons are introduced into a photomultiplier tube to generate a current signal, as the photon's energy is ultimately lost and defined to be zero.

Unlike previous measurement theories, it is not necessary to include measurement systems that must be treated quantum mechanically. If we define 'measurement' as above, we can separate the process of observing a quantum system from its environment. Thereby, we can overcome the difficulties of previous observation theories, such as where to place the Heisenberg cut that separates quantum systems from classical systems and whether the effect of 'consciousness' should be considered. If we define the measurement process in this way, we need not deal with the effects of the observation device, and therefore, open systems were not considered in this study.

This study also assumed a superposition of pure states in which each state has an orthonormal relationship. However, it is difficult to keep a quantum system in a pure state, and there is a certain cost involved in obtaining information about the single state [21]. In general measurements, a quantum system in a superposition state may transform into a mixed system, or the quantum system may be a mixed system that is not in a pure superposition state to begin with. These observation processes are usually described using a mixed density matrix. This study also required such handling in general measurements, and consequently, there could be situations where the states do not converge to one. How to handle such cases is shown in section 4.

1.4 Consistency with Born's Probability Law

In Section 1.2, energy eigenstates are assumed. In energy eigenstates, the energy of each state is determined in advance. When measuring a system in which such energy eigenstates are superposed, it is necessary to consider how the energy fluctuations occur and how one state is determined by the Born's probability law.

The overlay state before measurement is expressed as equation (11). Measurements act to select states on the system. Once subjected to this state selection, each following individual states $a_1|\psi_1\rangle, a_2|\psi_2\rangle, \cdots, a_m|\psi_m\rangle, \cdots$ are given energy by a measuring device.

Each state has an oscillation according to equation (7), and the measurement device also has quantum fluctuations. Therefore, when each state interacts with the measurement device, fluctuations occur in the energy received from the measurement device. At this time, the phase relationship between each time-varying state and the measurement device is determined haphazardly. This determines the magnitude of the fluctuation in the energy received from the measuring device probabilistically.

As mentioned above, the state $a_m|\psi_m\rangle$ with the smallest energy fluctuation magnitude ΔE_m is the state determined by this measurement. Therefore, the state selected by the measurement is also determined probabilistically.

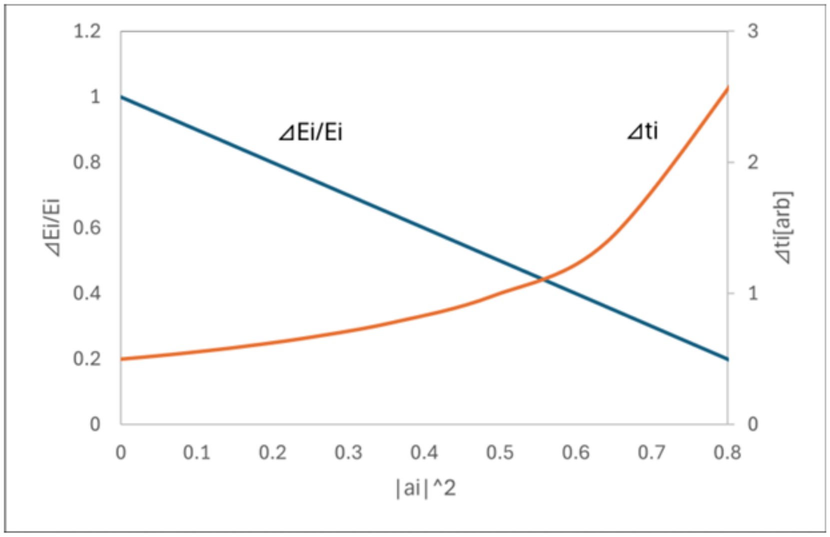

Figure 4: Square of expansion coefficients and fluctuations of energy and time

Measurement is not simply a disturbance, but acts to determine the state. According to quantum mechanics, the probability of a state being determined follows the Born rule. This study considers this in terms of the relationship between energy fluctuations and time fluctuations that occur during the measurement process.

The expectation value $\langle E_i \rangle$ of the energy of the state $|\psi_i\rangle$ can be written as follows using Born rule:

$$\langle E_i \rangle = |a_i|^2 E_i. \tag{13}$$

Here, E_i is the energy when the state is determined to be $|\psi_i\rangle$. Also, a_i is the expansion coefficient of E_i expanded in the energy basis, $0 \leq |a_i|^2 \leq 1$. During the measurement process, energy fluctuations occur in each state. Among these energy fluctuations, E_i is the maximum energy that the state $|\psi_i\rangle$ can have. Therefore, the width of the energy fluctuations ΔE_i that occur during the measurement process can be written as follows:

$$\Delta E_i = E_i - \langle E_i \rangle = (1 - |a_i|^2) E_i. \tag{14}$$

This relationship against $|a_i|^2$ and $\Delta E_i / E_i$ is shown by Figure 4. In this way, the energy fluctuation range ($\Delta E_i / E_i$) that can occur during the measurement process is inversely correlated, becoming smaller as $|a_i|^2$ becomes larger. Also, the time fluctuation width ($\Delta t_i \geq \hbar / 2\Delta E_i$) is inversely proportional to ΔE_i, so it increases as $|a_i|^2$ increases. Therefore, the state $|\psi_m\rangle$ with the largest $|a_m|^2$ will have the largest time fluctuation Δt_m and is expected to become the final measurement state.

1.5 Consistency with Previous Theories and Experiments

This study is consistent with the widely accepted interpretation of the energy-time uncertainty relation proposed by Mandelstam and Tamm, which involves the time scale of state establishment [17].

This situation is illustrated in Figure 5. As the energy is determined by observation, time fluctuation occurs, and the bra vector $a_m{}^*\langle\psi_m|$ reaches the furthest past $-\Delta t_m/2$. This $a_m{}^*\langle\psi_m|$ will become the final observation result. Such time fluctuation also occurs in the future. The state ket vectors $a_1|\psi_1\rangle, a_2|\psi_2\rangle, \cdots, a_m|\psi_m\rangle, \cdots$ reach their respective time fluctuation points. However, $a_1|\psi_1\rangle, a_2|\psi_2\rangle, \cdots$ do not go beyond $+\Delta t_m/2$, and hence, what remains in the end is only $a_m{}^*a_m\langle\psi_m|\psi_m\rangle$, which is already established in the braket state. Therefore, for the state to be established, a time duration Δt_m from $-\Delta t_m/2$ to $+\Delta t_m/2$ is required. This is consistent with the conventional interpretation above that the energy-time uncertainty relation indicates the time it takes for a state to be determined.

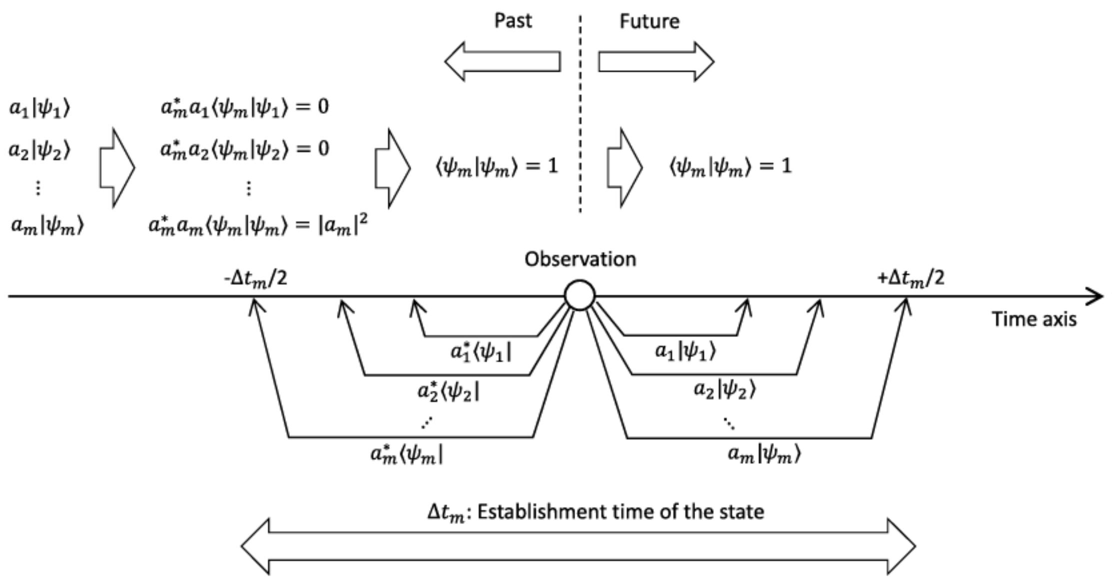

Figure 5: Reaching state vectors and establishment time of the state

Recently, research into the measurement process of quantum systems has progressed through the use of weak measurements proposed by Aharonov et al. [22]. Weak measurements are made without destroying the superposition state. In weak measurements, the energy of the quantum system being measured is not completely determined [22], and hence, the energy fluctuation ΔE_i of each quantum state would be large, while the time fluctuation Δt_i would be small.

Nevertheless, this study predicts that the state $|\psi_m\rangle$ with the smallest energy fluctuation ΔE_m and the largest time fluctuation Δt_m would be the most likely to result from the weak measurement. However, in weak measurements, the difference between these fluctuations is small, and hence, the variation in the results from each measurement is large. Aharonov et al. applied a time-symmetric 'two-state vector formulation' to weak measurement; in this formulation, future states as well as past states are to calculate the probability of the measurement result [8].

This study also considered elements that corresponded to Aharonov et al.'s theory. As shown in Figure 5, for a certain range into the future from the time of measurement, there exist many states $a_1|\psi_1\rangle, a_2|\psi_2\rangle, \cdots$ in addition to $a_m|\psi_m\rangle$, and hence, the state is not determined until the limit of the future time that these states can reach. In other words, the contraction of the quantum state is not complete until the state is determined. This appears to be the case for the two-state vector form, where a range of future states also influence the current state. Nevertheless, in this study, the state has already been selected by $a_m{}^*\langle\psi_m|$ which reaches the furthest past. Thus, even if multiple states exist in the range extending slightly into the future from the measurement point, the state to be determined has been selected at a past stage.

However, if the measurement does not sufficiently determine the energy of the quantum system, multiple states begin to coexist again and the superposition state is maintained. Even in such a situation, the state with the smallest energy fluctuation can be determined from the weak value of the observation at each time, and there is a difference in the probability of obtaining the weak value. The measurement result obtained most frequently from multiple weak measurements will be consistent with the result from a strong measurement.

In systems using superconducting qubits, which have extremely small energy dissipation, the capability to return to the superposition state is high even when a weak measurement is performed. This makes it difficult to determine the state in the manner of this study. Researchers have succeeded in directly observing various quantum states without determining them [23,24].

1.6 Wave Contraction in Single Electron Interference Apparatus

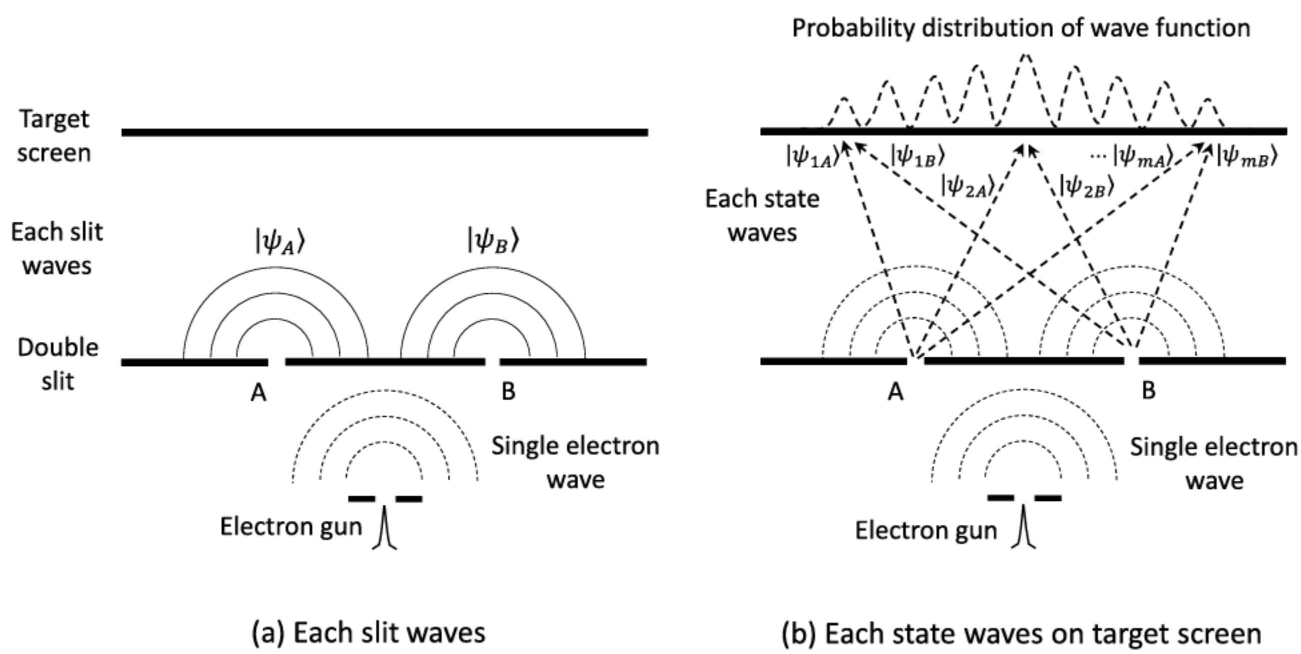

Figure 6: Single electron interference in double slit apparatus

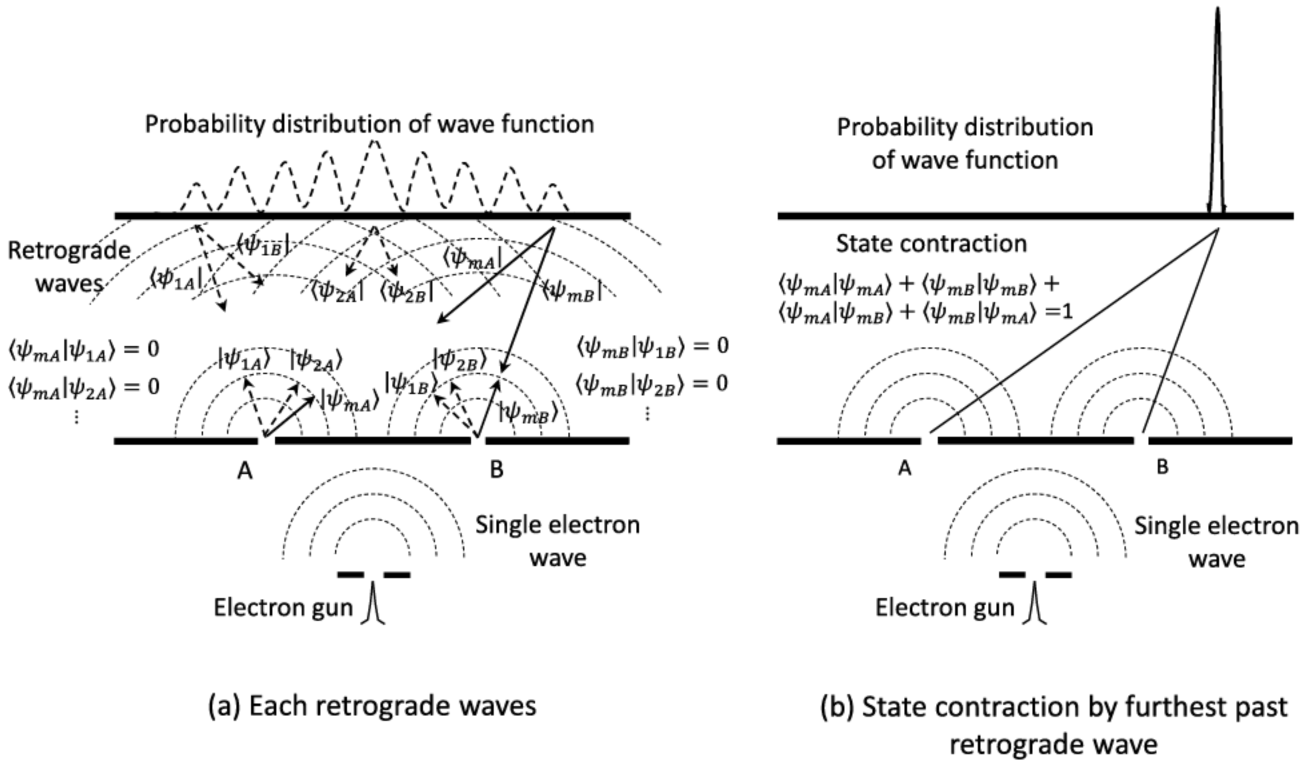

Figure 7: Wave contraction in single electron apparatus

The wave contraction mechanism in this study was determined by considering the famous single-electron interference at a double slit. Figure 6(a) shows a schematic of the experimental setup [25]. A single electron emitted from an electron gun travel through space as an electron wave, passes through the double slit, and splits into two electron waves $|\psi_A\rangle + |\psi_B\rangle$ which are omitted coefficients, that interfere with each other.

When this interference wave reaches the target screen, as shown in Figure 6(b), state waves $|\psi_{1A}\rangle + |\psi_{1B}\rangle$, $|\psi_{2A}\rangle + |\psi_{2B}\rangle$, $\cdots$, $|\psi_{mA}\rangle + |\psi_{mB}\rangle$, $\cdots$ are formed at the different arrival positions. These electron wave states interact with silver atoms on the target screen and determine their energy. Depending on the uncertainty range of this energy, namely ΔE_1, ΔE_2, $\cdots$, ΔE_m, $\cdots$, time fluctuations Δt_1, Δt_2, $\cdots$, Δt_m, $\cdots$ arise, in accordance with the energy-time uncertainty relation.

Since these state waves also fluctuate in the past direction, they generate time-reversed waves $\langle\psi_{1A}| + \langle\psi_{1B}|$, $\langle\psi_{2A}| + \langle\psi_{2B}|$, $\cdots$, $\langle\psi_{mA}| + \langle\psi_{mB}|$, $\cdots$ as shown in Figure 7(a). Among the time-reversed waves, the state with the smallest energy uncertainty ΔE_m has the largest time fluctuation Δt_m, and therefore this bra vector $\langle\psi_{mA}| + \langle\psi_{mB}|$ can reach the furthest into the past. As this bra vector $\langle\psi_{mA}| + \langle\psi_{mB}|$ combines with the components of the ket vectors $|\psi_{1A}\rangle + |\psi_{1B}\rangle$, $|\psi_{2A}\rangle + |\psi_{2B}\rangle$, $\cdots$,$|\psi_{mA}\rangle + |\psi_{mB}\rangle$, $\cdots$ at the furthest time point, the components orthonormal to it disappear, and finally $\langle\psi_{mA}|\psi_{mA}\rangle + \langle\psi_{mB}|\psi_{mB}\rangle + \langle\psi_{mA}|\psi_{mB}\rangle + \langle\psi_{mB}|\psi_{mA}\rangle = 1$ remains as shown in Figure 7(b). This represents the respective probability, and this is the physical mechanism by which the wave contraction upon observation.

In such an experimental setup, it may be possible to experimentally verify this theory, for example by observing the time-reversed waves coming from the target screen side in Figure 7(a). However, placing a measuring device on the path will block the time-progressing wave, so some ingenuity is required for observation.

1.7 Single Photon Detection in Mach-Zehnder Interferometer

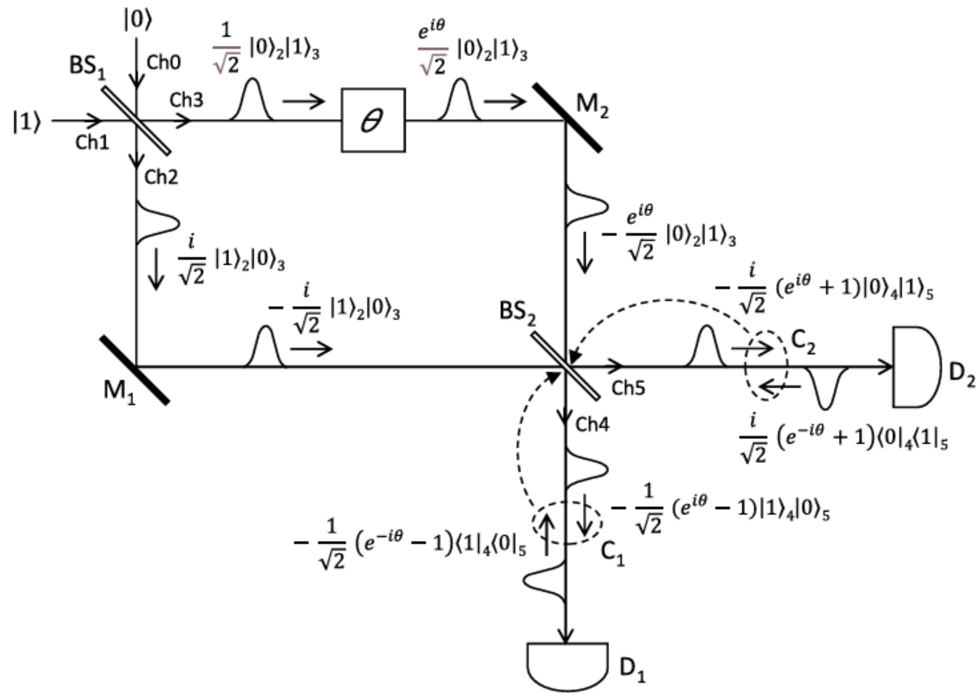

Figure 8: Single photon detection in Mach-Zehnder interferometer

In the Mach-Zehnder interferometer shown in Figure 8, it is known that interference occurs when a single photon is split into several paths by a beam splitter and these paths are focused onto another beam splitter by a mirror [26]. We used two symmetric and lossless beam splitters, BS_1 and BS_2, and let one photon enter from Ch1 of BS_1. Let this state be $|1\rangle$. Since zero photons are allowed to enter from Ch0, let this be $|0\rangle$. The unitary matrix of the beam splitter can be expressed as

$$U=\frac{1}{\sqrt{2}}\begin{pmatrix}1 & i\\ i & 1\end{pmatrix}. \tag{15}$$

The output of BS_1 is

$$|\mathrm{Ch2}\rangle=\frac{i}{\sqrt{2}}|1\rangle_2|0\rangle_3, \tag{16}$$

$$|\mathrm{Ch3}\rangle=\frac{1}{\sqrt{2}}|0\rangle_2|1\rangle_3. \tag{17}$$

A phase converter is placed on Ch3, which results in the following equation:

$$|\mathrm{Ch3}\rangle = \frac{e^{i\theta}}{\sqrt{2}}|0\rangle_2|1\rangle_3. \tag{18}$$

$|\mathrm{Ch2}\rangle$ and $|\mathrm{Ch3}\rangle$ underwent phase inversion and a sign change because of the perfectly reflecting mirrors M_1 and M_2, and the reflected waves were output by the beam splitter BS_2 as follows.

$$|\mathrm{Ch4}\rangle = -\frac{1}{\sqrt{2}}\left(e^{i\theta} - 1\right)|1\rangle_4|0\rangle_5, \tag{19}$$

$$|\mathrm{Ch5}\rangle = -\frac{i}{\sqrt{2}}\left(e^{i\theta} + 1\right)|0\rangle_4|1\rangle_5. \tag{20}$$

When these output waves were detected by detectors D_1 and D_2, their energy dispersion was reduced and the time uncertainty width increased. This led to the generation of the following time-reversed waves of the bra vector:

$$\langle\mathrm{Ch4}| = -\frac{1}{\sqrt{2}}\left(e^{-i\theta} - 1\right)\langle 1|_4\langle 0|_5, \tag{21}$$

$$\langle\mathrm{Ch5}| = \frac{i}{\sqrt{2}}\left(e^{-i\theta} + 1\right)\langle 0|_4\langle 1|_5. \tag{22}$$

At C_1 and C_2, where these time-reversed bra vectors combined with the time-forward ket vectors, the following equations, which provide the probabilities of obtaining a photon, hold:

$$C_1: \langle\mathrm{Ch4}|\mathrm{Ch4}\rangle = \frac{1}{\sqrt{2}}(1 - \cos\theta), \tag{23}$$

$$C_2: \langle\mathrm{Ch5}|\mathrm{Ch5}\rangle = \frac{1}{\sqrt{2}}(1 + \cos\theta). \tag{24}$$

In conventional quantum theory, these probabilities were calculated by multiplying the ket vector by its bra vector as a mathematical technique. In this study, however, they were obtained by combining the time-reversed bra vector with the ket vector as a physical process. These showed that the wave packet disappeared upon observation.

In the case of a single photon, the photon is detected by either detector D_1 or D_2. Now, consider the case where a photon is detected by detector D_1. Here, whether the photon is detected at D_1 or not is determined when the photon's path is selected as Ch4 or not at BS_2. Therefore, the bra-ket state of equation (23) that determines the state is formed at the stage of BS_2. At this time, the position of C_1 regresses to BS_2. Then, the time-reversed wave $\langle\mathrm{Ch4}|$ travels to BS_2 and erases $|\mathrm{Ch5}\rangle$, which is orthogonal to it. In this way, the wave packet contraction is completed. The result is similar if the photon is detected at D_2, in which case the position of C_2 regresses to BS_2.

Even in this system, it may be possible to experimentally verify this theory. For example, when observing a photon at D_1 in Figure 8, it may be possible to observe the time-reversed photon of equation (21) returning from D_1. However, even in this case, it is necessary not to interfere with the time-forward photon of equation (19) coming from BS_2.

1.8 Bidirectional Quantum Time and Unidirectional Macroscopic Time

Fluctuations in the quantum intrinsic time occurred both in the past and future directions and were symmetric with respect to time. However, as shown in Figures 5, the determined state evolved in unidirectional time. This was because the determined state did not fluctuate over time, and it followed the progression of 'macroscopic time'. However, why does macroscopic time progress in only one direction?

Dressel et al. investigated the statistical arrow of time for a quantum system being monitored by a sequence of measurements [27]. For a continuous qubit measurement example, they demonstrated that time-reversed evolution is always physically possible, provided that the measurement record is also negated. Despite this restoration of dynamical reversibility, a statistical arrow of time emerged, and it could be quantified by the log-likelihood difference between forward and backward propagation hypotheses.

Manikandan et al. generalised Dressel et al.'s discussion of a statistical arrow of time for continuous quantum measurements, and they showed that backward probabilities could be computed from a process similar to retrodiction from the time reversed final state [28]. Furthermore, they extended the definition of an arrow of time to ensembles prepared with pre- and post-selections, and they obtained a non-vanishing arrow of time in general.

In recent years, research on the origin of time has progressed. Rovelli argues that time is not a prerequisite for physical systems because time does not appear explicitly in quantum loop theory studies. He states that time is produced by state changes in spin networks in quantum loop theory and proposes that macroscopic time be treated as a thermodynamic state variable analogous to entropy [29]. Connes and Rovelli discussed the relationship between time and thermodynamics on the basis of a covariant quantum theory, and they introduced the concept of thermal time [30]. It is said that time does not originally exist, but is created by changes in physical systems.

Extending this idea, it is suggested that 'macroscopic time' arises from changes in macroscopic physical systems. Since such changes are statistically unidirectional, the macroscopic time associated with such changes is also thought to be unidirectional. This appears to be the reason for what we perceive as macroscopic time progressing in one direction.

1.9 Definitions for Non-Standard Terms

This study uses non-standard terms and concepts such as time-reversed bra vectors and bra-ket states. This section explains these definitions and concepts more precisely.

1.9.1 Time-Reversed Bra Vector

If we apply a time-reversal transformation to the fundamental equations of quantum mechanics and take the complex conjugate of the whole, we get the same form as the original equations (see equations (2) and (4)). The time-reversal vector is the solution of the time-reversal equation. This vector is the complex conjugate of the original and then transposed, changing the vector from a ket vector to a bra vector. The time evolution of the time-reversed bra vector is an antiunitary transformation (see equation (8)), describing the time evolution in the negative direction. The phase of the time-reversed bra vector is a complex conjugate of the phase of the original time-forward ket vector, so the sign of only the imaginary part is reversed, not the entire phase. This time-reversed bra vector is compatible not only with the non-relativistic Schrödinger equation, but also with the Dirac equation, which treats fermions relativistically, and the Klein-Gordon equation, which treats bosons relativistically, as shown in section 3.4 [14]. Also, the validity of treating the behavior of a single photon with the Schrödinger equation was also mentioned in section 3.

1.9.2 Bra-ket State

The bra-ket state is defined as the inner product of quantum states that are complex conjugates of each other. In quantum mechanics, such inner products have been used as a method for calculating the probability of each quantum state. However, this study considers that some bra-ket states exist as quantum states in certain situations. This study particularly deals with the inner product of the time-forward ket vector $|\psi_i(t)\rangle$ and the time-reversed bra vector $\langle\psi_i(t)|$ as below.

$$\langle\psi_i(t)|\psi_i(t)\rangle = \langle\psi_i|\psi_i\rangle. \tag{25}$$

The process by which this state is formed can be considered as shown in Figure 9. The state vector that changes from t_1 to t_0 is expressed as follows:

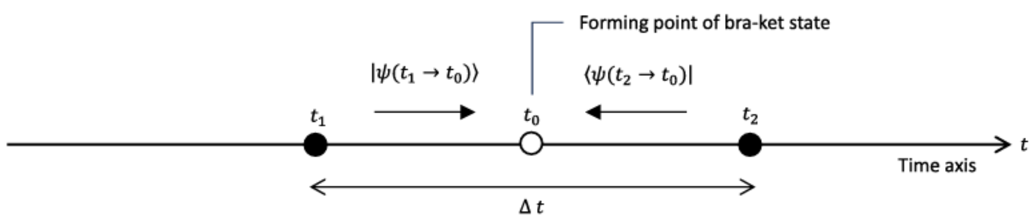

Figure 9: Nearby forming point of bra-ket state

$$|\psi_i(t_1 \to t_0)\rangle = e^{-\frac{i}{\hbar}\int_{t_1}^{t_0}\hat{H}tdt}|\psi_i(t_1)\rangle. \tag{26}$$

Similarly, the state vector that changes from t_2 to t_0 is

$$\langle\psi_i(t_2 \to t_0)| = \langle\psi_i(t_2)|e^{\frac{i}{\hbar}\int_{t_2}^{t_0}\hat{H}tdt}. \tag{27}$$

These form a bra-ket state at t_0 as follows:

$$\begin{aligned}\langle\psi_i(t_2\to t_0)|\psi_i(t_1\to t_0)\rangle &= \langle\psi_i(t_2)|e^{\frac{i}{\hbar}\int_{t_2}^{t_0}\hat{H}tdt}e^{-\frac{i}{\hbar}\int_{t_1}^{t_0}\hat{H}tdt}|\psi_i(t_1)\rangle \\ &= \langle\psi_i(t_2)|e^{\frac{i}{\hbar}\int_{t_2}^{t_0}\hat{H}tdt-\frac{i}{\hbar}\int_{t_1}^{t_0}\hat{H}tdt}|\psi_i(t_1)\rangle \\ &= \langle\psi_i(t_2)|e^{-\frac{i}{\hbar}\int_{t_1}^{t_2}\hat{H}tdt}|\psi_i(t_1)\rangle \\ &= \langle\psi_i(t_2)|e^{-\frac{i}{\hbar}(\hat{H}t_2-\hat{H}t_1)}|\psi_i(t_1)\rangle \\ &= \langle\psi_i(t_2)|e^{-\frac{i}{\hbar}(\hat{H}\Delta t)}|\psi_i(t_1)\rangle.\end{aligned} \tag{28}$$

If we set $\Delta t\to 0$, the above equation becomes

$$\begin{aligned}\langle\psi_i(t_2\to t_0)|\psi_i(t_1\to t_0)\rangle &= \langle\psi_i(t_0)|\hat{\mathbf{1}}|\psi_i(t_0)\rangle \\ &= \langle\psi_i(t_0)|\psi_i(t_0)\rangle \\ &= \langle\psi_i|\psi_i\rangle\end{aligned} \tag{29}$$

The bra-ket state thus formed does not change over time.

1.10 How does the time-reversed state vector start and lead to state contraction?

1.10.1 Boundary Conditions for the Time-Reversed State to Propagate Backward

If the time reversal occurs at t_0, the initial conditions can be determined at t_0. Since the state of this time-reversed quantum is the complex conjugate of the time-forward quantum, it starts from a state in which the sign of the imaginary part is reversed. In other words, if the phase of the time-forward quantum at t_0 is θ $(0\le\theta\le\pi)$, then the phase of the time-reversed quantum at t_0 is $-\theta$ (Figure 10). Furthermore, the real parts and squared absolute values of the wave functions ψ of both at t_0 are equal, and the magnitude and existence probability of the wave functions ψ are equal.

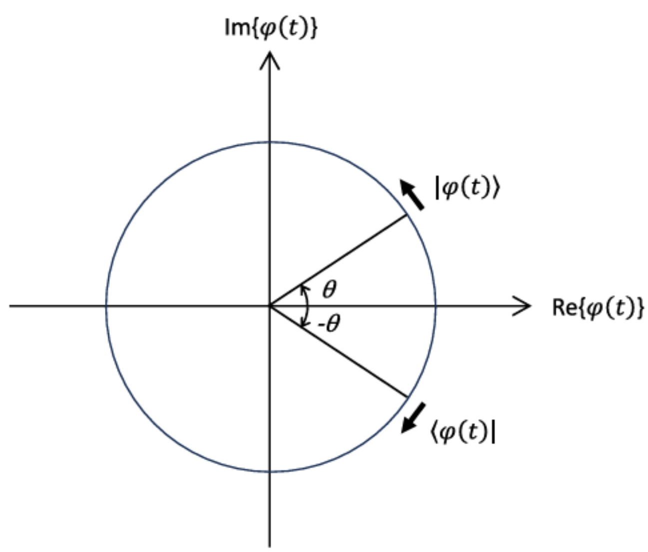

Figure 10: Phases of bra vector and ket vector

1.10.2 How does this Lead to State Contraction?

As shown in equation (11), when a superposition state represented by a linear combination of ket vectors is multiplied by a bra vector representing a single state as an inner product, due to the orthogonality between the states, only the inner product component between this bra vector and the ket vector that was originally in the same state remains. This allows us to describe the process by which one state remains from the superposition state as in equation (12). In this study, this process is considered as state contraction.

1.11 Experimental Possibilities for Distinguishing the Other Interpretations

1.11.1 Abbreviation of the Concept in this Study

To simplify the description, it may be better to give an abbreviation to the concept in this study. The essential concept of this study is time reversal due to time uncertainty. However, there are other theories that use time reversal like TI and TSVF. These can be called TRVFs (time reversed vector formalisms) including this study. To distinguish this study from others, this study is called 'BKSF (bra-ket state formalism)' below.

1.11.2 Experimental predictions that distinguish them from TI

In the TI, the phase θ_1 of the time-progressive wave (confirmation wave) and the phase θ_2 of the time-regressive wave (response wave) that establishes the state by being superimposed on it are in phase with each other, i.e., $\theta_1 = \theta_2$. On the other hand, in this study (BKSF), the phase θ_1 of the time-progressive wave and the phase θ_2 of the time-regressive wave are in a complex conjugate relationship, with only the sign of the imaginary part being inverted, i.e., $\theta_1 = -\theta_2$. If we could somehow measure these phases θ_1, θ_2, or the phase difference $\theta_1 - \theta_2$, we could distinguish between these interpretations.

1.11.2 Experimental Predictions that Distinguish from TSVF

Figure 11 shows a comparison between TSVF and BKSF.

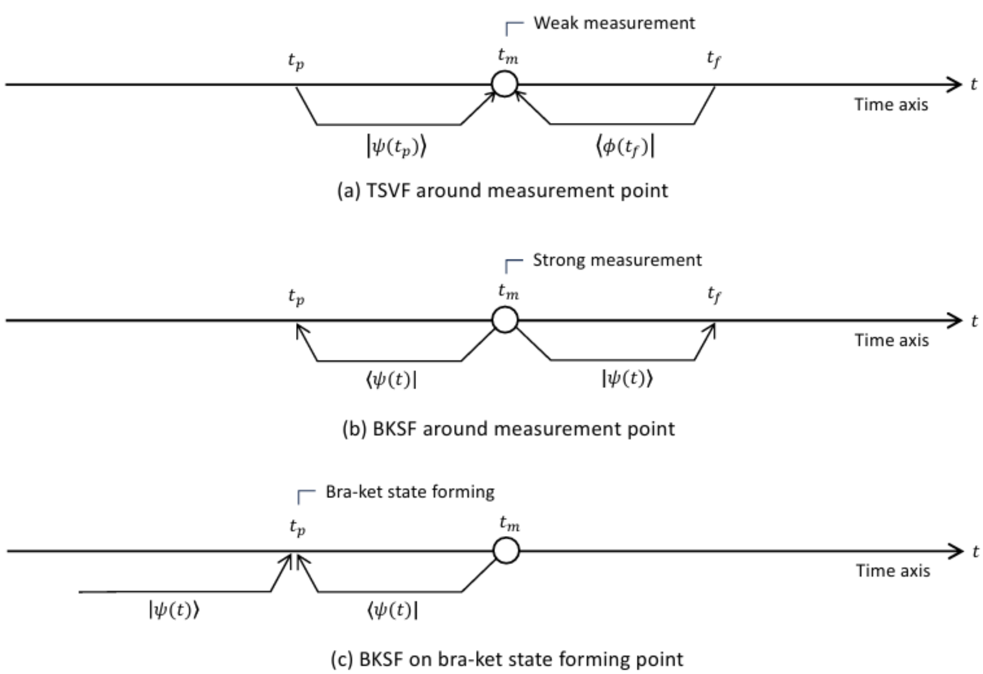

Figure 11: Comparison of TSVF and BKSF(this study)

As shown in Figure11(a), TSVF defines the state vector at t_m(measurement point) by the state vector at t_p(past) and the state vector at t_f(future). TSVF calculates the expected value of the physical quantity A as follows:

$$A_w = \frac{\langle\phi|A|\psi\rangle}{\langle\phi|\psi\rangle}. \tag{30}$$

This result is consistent with the average of multiple weak measurements at t_m. In the BKSF shown in Figure 11(b), if a normal measurement (here called a strong measurement) is performed on t_m, the state vector can go either in the t_p direction or the t_f direction due to the time uncertainty.

Comparing the two formalisms, we can see that the two state vectors act in the opposite directions. The two state vectors of TSVF are acting on t_m from the past t_p and future t_f, and two state vectors of BKSF pointing from t_m to the past and future. However, these differences could not be directly distinguished experimentally. This is because, as shown in Figure 11(c), the state vectors of BKSF come from the past and future to form a bra-ket state at t_p. This is the same situation as TSVF. So, it seems difficult to distinguish between the two interpretations' vectors.

However, the two state vectors of the TSVF appear prominently in weak measurements, and it is possible to observe them in weak measurements that do not completely determine the state. On the other hand, the time-reverse waves in BKSF appear more clearly when strong measurements are made to confirm the state. Therefore, if time-reverse waves can be observed when strong measurements are made, it supports BKSF. However, when weak measurements are made, the situation shown in BKSF becomes closer to the weak measurement situation and may be indistinguishable from the time-reversing state vector in TSVF.

2. QFT-based Interpretation of the Spatial Contraction of a Wave Packet upon Observation [31]

The nature of the wave function has been extensively debated since the formulation of quantum mechanics [2]. If this function indeed faithfully represents the behavior of elementary particles such as electrons, then clarifying its nature becomes equivalent to understanding the ontological status of the particles themselves. In quantum field theory, elementary particles are interpreted as excited states of the vacuum, which indicates that the wave function in quantum mechanics may be a manifestation of vacuum-field energy. This perspective further motivates a reexamination of long-standing problems, including wave packet collapse upon measurement, which remains a central topic of debate in quantum mechanics [3]. The present study proposes that this collapse is associated with vacuum-field energy. However, because the vacuum energy density is spatially uniform, it contributes merely a constant term to the Hamiltonian of a quantum system. This constant contribution alters only the total phase in the time evolution of the time evolution of the wave function and does not modify the probability density or spatial distribution. Consequently, it cannot account for spatial contraction.

Unlike purely quantum-mechanical approaches, some studies have incorporated general-relativistic effects into the analysis of the wave function. One such study incorporated the cosmological constant Λ into the vacuum energy to describe the wave function in curved spacetime [32]. Within this framework, if $\Lambda > 0$ (de Sitter vacuum), the resulting potential is repulsive, leading to wave function diffusion. Conversely, if $\Lambda < 0$ (anti-de Sitter vacuum), the potential is attractive, and resulting in wave function collapses. However, because these effects induce the expansion or contraction of space itself, they do not explain the contraction of the wave function relative to that of space.

Meanwhile, other studies have examined whether wave packet collapse upon observation can be attributed to vacuum pressure. In Diósi's gravitational collapse theory, differences in gravitational energy between superposed states perturb the gravitational field of the vacuum, there by inducing local collapse of the wave function [33]. Nevertheless, because this mechanism is inherently probabilistic, it cannot adequately explain why collapse occurs immediately upon observation.

A further line of inquiry explores whether vacuum fluctuations may contribute to the effective contraction of the wave function. Notably, because the vacuum is not perfectly uniform, it exhibits quantum fluctuations. When these fluctuations couple to the wave function, they generate an effective potential through a mean-field contribution. If this potential functions as a binding self-interaction, it constrains the spatial spread of the wave function. Notably, this potential does not represent vacuum pressure but instead corresponds to an effective nonlinear term arising from interactions with the vacuum field [34]. However, even this mechanism does not fully account for the contraction triggered by observation.

An alternative explanation involves post-measurement vacuum reconstruction [35], wherein the measurement of a particle's state induces a slight modification in the local structure of the vacuum field, thereby causing the vacuum expectation value to shift to a different state. This phenomenon, referred to as "local vacuum relocation," reflects a response of quantum electromagnetic fields, rather than a physical collapse of the spatial probability density of the wave function. Consequently, it just implies that the local vacuum configuration is determined by the observed outcome.

In Chapter 1, this study investigated the mechanism underlying the observation-induced contraction of the state vector through the formation of bra-ket states arising from time-reversed waves [4]. Although this framework successfully explains the contraction of multiple superposed quantum states into a single state upon observation, it does not address the subsequent spatial contraction of that state, which is defining feature of wave-packet collapse. The bra-ket states described in this study correspond mathematically to the inner product of the bra and ket vectors. In Dirac notation, this expression corresponds to the spatial integral of the product of mutually complex-conjugate wave functions. However, the physical process through which this integral is realized and the spatially extended wave function becomes contracted remains unclear. Consequently, a comprehensive account of wave-packet collapse requires clarification of the mechanism underlying spatial contraction. This study provides such an account by demonstrating that spatial collapse arises spontaneously when the wave function is represented in terms of vacuum energy within the framework of quantum field theory.

2.1 Space Contraction Induced by Vacuum Energy

The previous section explained that the process of quantum state contraction; however, spatial contraction has not yet occurred, and wave packet collapse therefore remains incomplete. This section explains how the space contraction occurs.

The wave function ψ, as formulated in the Schrödinger equation, is interpreted as an excitation of vacuum energy. If this vacuum energy were released, the energy associated with ψ would decrease, resulting in a contraction of the spatial distribution of $\psi(t)$. However, such contraction does not occur before observation because the time evolution of $\psi(t)$ is governed by the unitary transformation $U = e^{-\frac{i\hat{H}t}{\hbar}}$. Under these conditions, $\psi(t)$ continues to propagate while being excited by vacuum energy, thereby preventing any contraction of its spatial extent. Further, upon observation, the state collapses into the bra-ket form $\langle \psi_i \mid \psi_i \rangle$, which terminates the unitary time evolution governed by $U = e^{-\frac{i\hat{H}t}{\hbar}}$, as defined in (7). This transition can be clarified more precisely by examining the Hamiltonian of the state vector. Notably, the total Hamiltonian $\hat{H}$ comprises the free-particle Hamiltonian $\hat{H}_0$ and the vacuum energy operator $\hat{V}$:

$$\hat{H} = \hat{H}_0 + \hat{V}. \tag{31}$$

Accordingly, the time evolution of the state vector is governed by the following by unitary transformation:

$$|\psi(t)\rangle = e^{-\frac{i(\hat{H}_0+\hat{V})t}{\hbar}}|\psi_0\rangle. \tag{32}$$

Within this framework, the vacuum energy operator $\hat{V}$ modifies only the phase of the state vector $|\psi(t)\rangle$. Upon observation, however, the state is projected into its bra-ket form. In this representation, the time-evolution factor vanishes, and the contribution from the vacuum energy component of the Hamiltonian consequently disappears:

$$\langle \psi(t)|\psi(t)\rangle = \langle \psi_0|e^{\frac{i(\hat{H}_0+\hat{V})t}{\hbar}} e^{\frac{-i(\hat{H}_0+\hat{V})t}{\hbar}}|\psi_0\rangle = \langle \psi_0|\psi_0\rangle \tag{33}$$

This operation also eliminates the oscillations of $|\psi(t)\rangle$ and $\langle \psi(t)|$, which originally arise from the vacuum energy states $|0\rangle$ and $\langle 0|$. Consequently, the wave function $\psi(t)$ releases energy, and its spatial extent correspondingly contracts. This process constitutes the spontaneous collapse mechanism of the wave packet.

The bra-ket notation introduced above is a Dirac shorthand, formally expressed as

$$\langle \psi|\psi\rangle = \int \psi^* \psi dr. \tag{34}$$

If the wave function ψ represents an oscillation of a vacuum-energy quantum, then the bra-ket state $\langle \psi|\psi\rangle$ corresponds to a stationary state wherein such oscillations have ceased. According to (9), this relation signifies the compression of multiple superposed states into a single state. However, this contracted state does not cease to exist. The integral in (34) remains unchanged, and the wave function ψ persists in a spatially extended configuration. Wave packet collapse therefore remains incomplete at this stage. To fully account for such collapse, the spatial domain appearing in (34) must likewise undergo spontaneous contraction. Thus, beyond observation-induced state contraction, spatial contraction must also be addressed to comprehensively explain wave packet collapse.

In general, a physical system evolves along a trajectory that minimizes its action integral, thereby reducing its energy. Within this framework, observation-induced wave packet collapse is interpreted as a result of releasing the zero-point vacuum energy stored in the spatial integral.

In quantum field theory, this energy corresponds to the wave function regarded as an excitation of the vacuum state. Accordingly, the state vector of the wave function $\psi(x)$ can be expressed by applying the field operator $\hat{\psi}(x)^\dagger$ to the vacuum state $|0\rangle$ [36]:

$$|\psi\rangle = \int d^3x |\psi(x)\rangle \hat{\psi}(x)^\dagger |0\rangle. \tag{35}$$

Substituting this, expression into (34) yields

$$\begin{aligned}\langle\psi|\psi\rangle &= \int d^3x \langle 0|\hat{\psi}(x)\psi(x)^*\psi(x)\hat{\psi}(x)^\dagger|0\rangle \\ &= \int d^3x |\psi(x)|^2 \langle 0|\hat{\psi}(x)\hat{\psi}(x)^\dagger|0\rangle. \end{aligned} \tag{36}$$

The state field operators $\hat{\psi}(x)^\dagger$ and $\hat{\psi}(x)$ may be expanded in terms of the creation and annihilation operators ${a_p}^\dagger$ and a_p as [36]:

$$\hat{\psi}(x)^\dagger = \int \frac{d^3p}{(2\pi)^3} {a_p}^\dagger e^{-ip\cdot x}, \tag{37}$$

$$\hat{\psi}(x) = \int \frac{d^3p}{(2\pi)^3} a_p e^{ip\cdot x}. \tag{38}$$

Using these operator relations, the term $\langle 0|\hat{\psi}(x)\hat{\psi}(x)^\dagger|0\rangle$ appearing in the integrand on the right-hand side of (36) can be reformulated as

$$\langle 0|\hat{\psi}(x)\hat{\psi}(x)^\dagger|0\rangle = \int \frac{d^3p}{(2\pi)^6} \langle 0|0\rangle. \tag{39}$$

Accordingly, (36) assumes the following form:

$$\langle\psi|\psi\rangle = \int \left[|\psi(x)|^2 \int \frac{d^3p}{(2\pi)^6} \langle 0|0\rangle \right] d^3x. \tag{40}$$

In this formulation, the term $\int \frac{d^3p}{(2\pi)^6} \langle 0|0\rangle$ within the spatial integral scales proportionally with the vacuum-state inner product $\langle 0|0\rangle$ across the region.

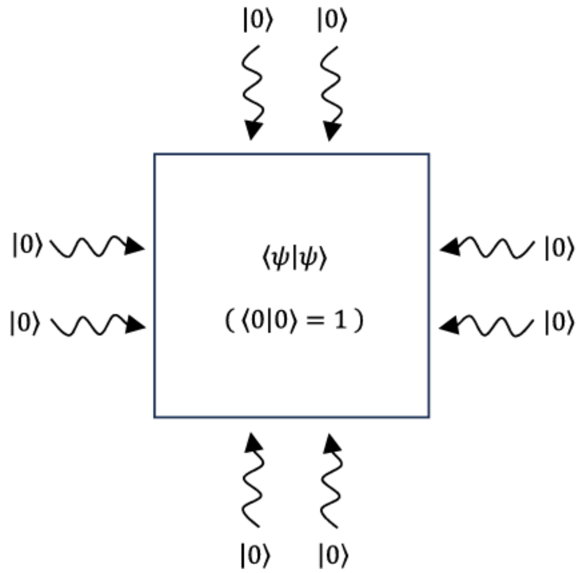

Figure 12: Bra-ket state subjected to compressive force from a vacuum field

Because each vacuum state $|0\rangle$ carries a zero-point fluctuation energy characteristic of a harmonic oscillator, expanding the spatial domain of integration in (40) increases the energy associated with the defined state $\langle\psi|\psi\rangle$. However, because physical systems inherently evolve toward lower-energy configurations, the spatial domain in (40) over which the state is defined is thus expected to undergo spontaneous contraction. Using the vacuum wave function of the harmonic oscillator, we obtain

$$\psi_0(x) = \left(\frac{\omega}{\pi\hbar}\right)^{\frac{1}{4}} e^{-\frac{\omega}{2\hbar}x^2}. \tag{41}$$

Using this expression, $\langle 0|0\rangle$in (40) is derived as

$$\langle 0|0\rangle = \int_{-\infty}^{-\infty} d\,x|\psi_0(x)|^2 = \left(\frac{\omega}{\pi\hbar}\right)^{\frac{1}{2}} \int_{-\infty}^{\infty} d\,x e^{-\frac{\omega}{\hbar}x^2} = 1. \tag{42}$$

Because $\langle 0|0\rangle$in (40) equals one, the contribution associated with vacuum-field fluctuations is eliminated. Accordingly, $\langle\psi|\psi\rangle$ in (40) no longer experiences pressure from the internal vacuum states $|0\rangle$ and $\langle 0|$ but remains subject to pressure from the external vacuum, as illustrated in Figure 12.

This vacuum-induced pressure has been experimentally verified as the Casimir effect [37,38].

2.2 Contraction Force Induced by Vacuum Energy

The force with which this vacuum energy contracts the wave packet domain can be determined using a procedure analogous to that employed for the Casimir force. In this section, we adopt calculation method proposed by Gee [39].

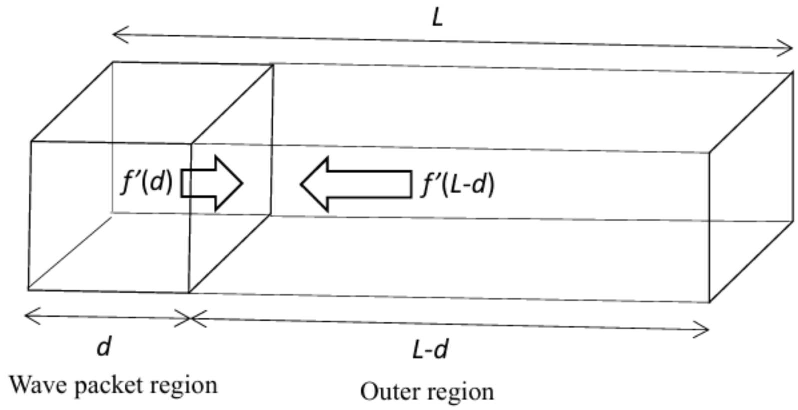

Figure 13: Forces acting on the wave packet domain field

Let us consider the one-dimensional model depicted in Figure 13. In this framework, the width of the wave packet region is denoted by d, while the total one-dimensional extent encompassing this region is denoted by L. Under this setting, the vacuum fluctuation energy per unit area, E, is expressed $E = f(d) + f(d-L)$. The fluctuation modes confined within d are then expressed as follows, using integers $n = 1, \ldots, \infty$:

$$k_n = \frac{n\pi}{d}. \tag{43}$$

The corresponding vacuum fluctuation energy $f(d)$ inside the wave packet region is expressed as

$$f(d) = \frac{\hbar c}{2}\sum_{n=1}^{\infty} k_n = \frac{\pi\hbar c}{2d}\sum_{n=1}^{\infty} n. \tag{44}$$

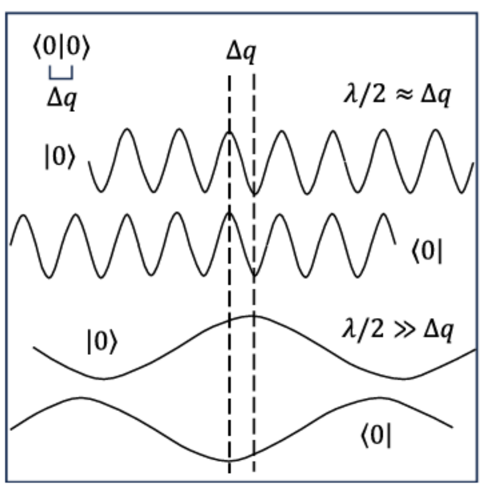

Figure 14: Cancellation of vacuum fluctuations with position uncertainty Δq

Although the bra-ket state $\langle\psi|\psi\rangle$ is formed, $\langle\psi|$ and $|\psi\rangle$ do not coincide with space exactly because of their relative position uncertainty Δq. The associated $\langle 0|$ and $|0\rangle$ states likewise do not coincide with space exactly; consequently, these vacuum fluctuations fail to form perfectly inverse phases, as illustrated in

Figure 14. Components with wavelength λ satisfying $\lambda/2 \gg \Delta q$ approach the inverse phase condition and are effectively canceled, whereas high-frequency components with smaller wavelengths satisfying $\lambda/2 \approx \Delta q$ approximately in phase and therefore persist in certain cases. These residual components within the bra-ket state $\langle\psi|\psi\rangle$ generate forces that oppose external forces. Consequently, external high-frequency components with wavelengths satisfying $\lambda/2 \approx \Delta q$ contribute negligibly to the compressive force that acting on the wave packet. In the following derivation, we introduce a factor $e^{-\Delta q k_n/\pi}$ to suppress the high frequency components. This factor suppresses contributions from oscillatory modes with $k_n \gg \frac{\pi}{\Delta q}$. Upon incorporating this factor, (44) becomes,

$$\begin{aligned} f(d) &= \frac{\pi\hbar c}{2d}\sum_{n=1}^{\infty} n\, e^{-\Delta q k_n/\pi} \\ &= \frac{\pi\hbar c}{2d}\sum_{n=1}^{\infty} n\, e^{-\Delta q n/d} \\ &= -\frac{\pi\hbar c}{2}\frac{\partial}{\partial\Delta q}\sum_{n=1}^{\infty} e^{-\Delta q n/d} \\ &= -\frac{\pi\hbar c}{2}\frac{\partial}{\partial\Delta q}\frac{1}{1-e^{-\Delta q/d}} \\ &= \frac{\pi\hbar c}{2d}\frac{e^{\Delta q/d}}{(e^{\Delta q/d}-1)^2}. \end{aligned} \tag{45}$$

For small Δq, suppressing the vibration mode of $k_n \gg \frac{\pi}{\Delta q}$ yields

$$f(d) = \pi\hbar c\left[\frac{d}{2\Delta q^2} - \frac{1}{24d} + \frac{\Delta q^2}{480d^3} + O(\Delta q^4/d^5)\right]. \tag{46}$$

The force F that compresses the wave packet region equals the difference between the vacuum forces in the outer and inner regions. Considering $\Delta q \ll d$, it is represented as:

$$\begin{aligned} F &= -\frac{\partial E}{\partial d} \\ &= -\{f'(d) + f'(L-d)\} \\ &= -\pi\hbar c\left[\left(\frac{1}{2\Delta q^2} + \frac{1}{24d^2} + \cdots\right) + \left(-\frac{1}{2\Delta q^2} - \frac{1}{24(L-d)^2} + \cdots\right)\right] \\ &\approx -\frac{\pi\hbar c}{24}\left[\frac{1}{d^2} - \frac{1}{(L-d)^2}\right]. \end{aligned} \tag{47}$$

For $L \gg d$, this becomes

$$F = -\frac{\pi\hbar c}{24d^2}. \tag{48}$$

This expression represents the force that compresses the wave packet in the one-dimensional model.

2.3 The Convergence of Integral in Bra-ket State

In this section, we examine how the integral in (36) can be converged. Based on (42), (40) can be reformulated as

$$\langle\psi|\psi\rangle = \int \left[|\psi(x)|^2 \int \frac{d^3p}{(2\pi)^6}\right] d^3x. \tag{49}$$

From the perspective of existence probability, this expression must satisfy

$$\langle\psi|\psi\rangle = \int |\psi(x)|^2 d^3x = 1. \tag{50}$$

Therefore, for proper normalization, the integral $\int \frac{d^3p}{(2\pi)^6}$ in (49) must equal unity. This requirement is supported by the following transformation. In the canonical quantization of fermionic fields, the following relation holds [36]:

$$\{\hat{\psi}_\alpha(x), \hat{\psi}_\beta(y)^\dagger\} = \delta_{\alpha\beta}\delta^{(3)}(x-y). \tag{51}$$

This anticommutation relation can be expressed as

$$\hat{\psi}_\alpha(x)\hat{\psi}_\beta(y)^\dagger = \delta_{\alpha\beta}\delta^{(3)}(x-y) - \hat{\psi}_\beta(y)^\dagger\hat{\psi}_\alpha(x). \tag{52}$$

Taking the vacuum expectation value yields

$$\langle 0|\hat{\psi}_\alpha(x)\hat{\psi}_\beta(y)^\dagger|0\rangle = \delta_{\alpha\beta}\delta^{(3)}(x-y) - \langle 0|\hat{\psi}_\beta(y)^\dagger\hat{\psi}_\alpha(x)|0\rangle. \tag{53}$$

Because $\hat{\psi}_\alpha(x)|0\rangle = 0$, the second term on the right-hand side vanishes, and (53) reduces to

$$\langle 0|\hat{\psi}_\alpha(x)\hat{\psi}_\beta(y)^\dagger|0\rangle = \delta_{\alpha\beta}\delta^{(3)}(x-y). \tag{54}$$

Here, $\delta^{(3)}(x-y)$ on the right-hand side becomes ill-defined in the same-point limit $y \to x$. However, in the bra-ket state of (36), the bra and ket are separated by a distance Δq. To represent this state, (54) can be rewritten as follows:

$$\langle 0|\hat{\psi}(x)\hat{\psi}(x)^\dagger|0\rangle = \delta^{(3)}(\Delta q). \tag{55}$$

Substituting this result into (36), and noting that $\delta^{(3)}(\Delta q)$ closes to unity upon integration with $\Delta q \to 0$, yields

$$\langle\psi|\psi\rangle = \int \left[|\psi(x)|^2 \delta^{(3)}(\Delta q)\right] d^3x \to 1. \tag{56}$$

This establishes the existence probability of the state. It also explains the mechanism by which the wave packet contracts once the state is determined through observation.

2.4 Experimental Verification

One possible experimental verification of this theory would involve detecting weak response waves generated when vacuum pressure compresses the wave packet. Such a response wave is expected to manifest as a weak electromagnetic pulse.

3. Interpretation of Simultaneous Correlation in Quantum Entanglement with Retro-Causality [14]

The long-range correlation without transmission time between two entangled quanta is a difficult problem to interpret because it violates the requirements of the theory of relativity. This study attempts to explain this phenomenon using quantum time reversal.

It has been shown by Hodgson that the time evolution of the localized photon state can be treated by quantum mechanics [40]. Hawton also developed photon quantum mechanics in real Hilbert space [41]. Southall shows that the state of a localized photon can be treated by the Schrödinger equation, and the photons that travel forwards and backwards in time require twice of the Hilbert space depending on the sign of the wave number vector k [42].

This paper considers the kinetic energy H_{dyn} as the Hamiltonian, the localized photon state can be treated by the Schrödinger equation is justified [42].

3.1 An Example of Estimating the Time Reversal Distance of Photons in the Atmosphere

As described above, the width Δt of the time reversal is defined by the uncertainty relationship between time and energy $\Delta E \Delta t \geq \frac{\hbar}{2}$. Therefore, the magnitude of Δt depends on the defined range of energies ΔE of the system.

For example, the wavelength λ of a helium-neon laser, which is proposed to be adopted as the standard wavelength, and its relative uncertainty value α are [43]:

$$\lambda = 632.9908[\text{nm}] \tag{57}$$

$$\alpha = 1.5 \times 10^{-6} \tag{58}$$

The uncertainty in the width of the energy of photons ΔE of this laser is as follows:

$$\Delta E = \frac{ch}{\lambda - \alpha\lambda} - \frac{ch}{\lambda} = \frac{ch\alpha}{\lambda(1-\alpha)}. \tag{59}$$

Here, c is the speed of light and h is the Planck constant. The uncertainty in the width of the time Δt is

$$\Delta t \geq \frac{\hbar}{2\Delta E} = \frac{\hbar\lambda(1-\alpha)}{2ch\alpha} = 1.12 \times 10^{-10}[\text{s}]. \tag{60}$$

When a photon travels a distance ΔL during the time Δt, the distance is given as

$$\Delta L = c \times \Delta t \geq 3.36 \times 10^{-2}[\mathrm{m}]. \quad (61)$$

However, in special relativity, the time t_{obj} experienced by an object traveling in a system moving at a velocity v is related to the time t_{stat} in a stationary system by

$$t_{obj} = \frac{\left(1 - \frac{v}{c}\right)}{\sqrt{1 - \frac{v^2}{c^2}}} t_{stat}. \quad (62)$$

Therefore, the uncertainty in the width of the time Δt_{stat} of the quantum traveling at the speed v is given as follows for the stationary system:

$$\Delta t_{stat} = \frac{\sqrt{1 - \frac{v^2}{c^2}}}{\left(1 - \frac{v}{c}\right)} \Delta t_{obj}. \quad (63)$$

Since this quantum is a photon traveling in the atmosphere, its velocity v is about 0.028% slower than the velocity of light c in vacuum due to the dielectric constant of the atmosphere. Namely,

$$\frac{v}{c} \approx 0.99972. \quad (64)$$

Thus, Δt_{stat} becomes

$$\Delta t_{stat} \approx 84.5 \Delta t_{obj}. \quad (65)$$

Hence, the uncertainty in the width of time of photons traveling in the atmosphere is about 84.5 times larger in the stationary system. Therefore, the distance ΔL_{stat} that a photon of the above laser travels in the stationary system when its own time uncertainty width expands to Δt_{stat} is

$$\Delta L_{stat} \approx 84.5 c \Delta t_{obj} \geq 2.84[\mathrm{m}]. \quad (66)$$

In order to demonstrate how estimate its practical range correlation length, the energy certainty of a laser beam with high wavelength stability is used as an example. However, if the uncertainty of the photon energy becomes almost zero due to the determination of the state, the correlation length can become as large as desired. Also, if it is in a vacuum, v→ c, so this length becomes infinite from equations (63) to (66).

In experiments employing photons in this way, the range covered by the time uncertainty width could overwhelm the experimental system.

This shows that there is a relationship between the certainty of the observed photon energy and the distance that quantum entanglement can reach. This relationship only specifies the lower limit, not the upper limit, so it does not show that there is a clear experimental upper limit to the distance that quantum entanglement can reach. However, experimental trends may be found, such as the shorter the distance that quantum entanglement can reach for photons with large energy dispersion, and the entanglement distance may tend to be shorter for photons traveling in a medium such as an optical fiber than in a vacuum.

3.2 Causality in the Aspect's Experiment

Assuming the above-mentioned time-reversal state, the experimentally confirmed EPR correlation can be explained in a manner consistent with the special relativity. For this, the following causal law that travels backward in time is considered.

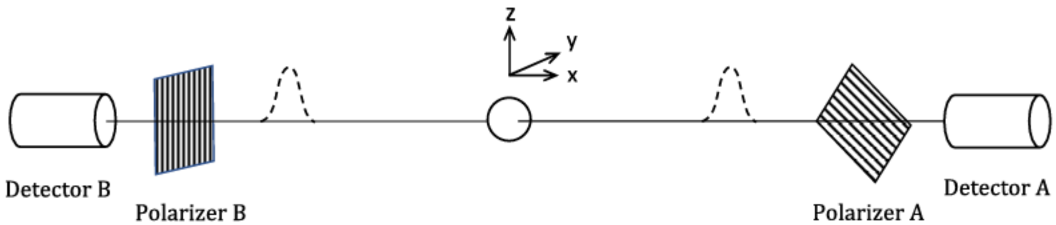

Figure 15: Aspect's experiment that violates the Bell's inequality

Figure 15 illustrates Aspect's experimental system and shows that the correlation between the polarization states of two photons violates Bell's inequality [13,45]. In this experiment, the violation of Bell's inequality cannot be explained unless the two photons in the entangled state are assumed to be instantaneously transmitted from one side to the other. This has been conventionally discussed as a problem that denies local reality.

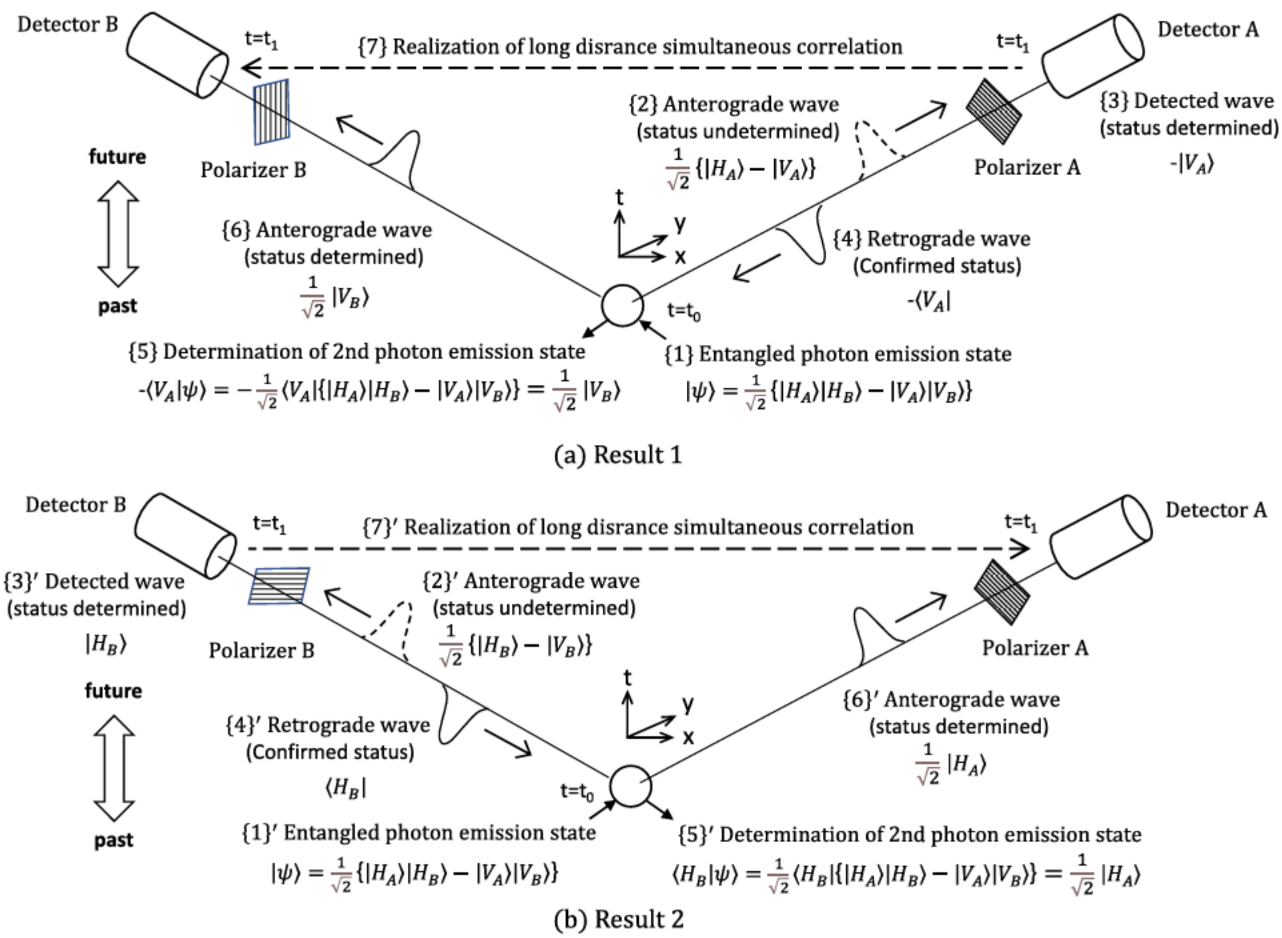

Figure 16: Interpretation of backward causality in Aspect's experiment

This is explained using Figure 16 as follows: Figure 16(a)(b) depicts the motion of photons in space time. In the figure, the top is the future, while the bottom is the past. The pair of photons emitted from the atom at time $t = t_0$ have entangled states {1} and {1}' that are expressed as

$$|\psi\rangle = \frac{1}{\sqrt{2}}\{|H_A\rangle|H_B\rangle - |V_A\rangle|V_B\rangle\}. \tag{67}$$

Here, $|H_A\rangle$ represents the photon that is horizontally polarized and flies toward detector A, $|V_B\rangle$ represents vertically polarized photon toward detector B, and so on.

Figure 16(a) displays the result of obtaining a vertically polarized state in detector A. The photon travels to detector A as the time anterograde wave {2} has an undetermined status $\frac{1}{\sqrt{2}}\{|H_A\rangle - |V_A\rangle\}$. The photon passes through polarizer A, and its status is determined by detector A. If the photon's status {3} is determined as $-|V_A\rangle$ at time $t = t_1$, it generates the time retrograde wave {4} of $-\langle V_A|$ because of the uncertainty of time. When this time retrograde wave returns to the original emitted atom, the polarization state of the 2nd photon emission {5} is determined as

$$-\langle V_A|\psi\rangle = \frac{1}{\sqrt{2}}\langle V_A|\{|H_A\rangle|H_B\rangle - |V_A\rangle|V_B\rangle\} = \frac{1}{\sqrt{2}}|V_B\rangle. \tag{68}$$

The time anterograde wave {6} with respect to the polarization state of $\frac{1}{\sqrt{2}}|V_B\rangle$ is emitted toward detector B.

Since this result is obtained at time $t = t_1$ at detector B, the determination of the state at detector A at time $t = t_1$ seems to be instantaneously transmitted to detector B {7}.

Figure 16(b) displays the result of obtaining a horizontally polarized state in detector B. The photon travels to detector B as the time anterograde wave {2}' has an undetermined status $\frac{1}{\sqrt{2}}\{|H_B\rangle - |V_B\rangle\}$. The status of the photon is modified by polarizer A and is determined by detector A. If its status {3}' is determined as $|H_B\rangle$ at time $t = t_1$, it generates the time retrograde wave {4}' of $\langle H_B|$ because of the uncertainty of time. When this time retrograde wave returns to the original emitted atom, the polarization state of the 2nd photon emission {5}' is determined as

$$\langle H_B|\psi\rangle = \frac{1}{\sqrt{2}}\langle H_B|\{|H_A\rangle|H_B\rangle - |V_A\rangle|V_B\rangle\} = \frac{1}{\sqrt{2}}|H_A\rangle. \tag{69}$$

The time anterograde wave {6}' with respect to the polarization state of $\frac{1}{\sqrt{2}}|H_A\rangle$ is emitted toward detector A. Since this result is obtained at time $t = t_1$ at detector A, the determination of the state at detector B at time $t = t_1$ seems to be instantaneously transmitted to detector A {7}'.

3.3 Compatibility with Special Relativity

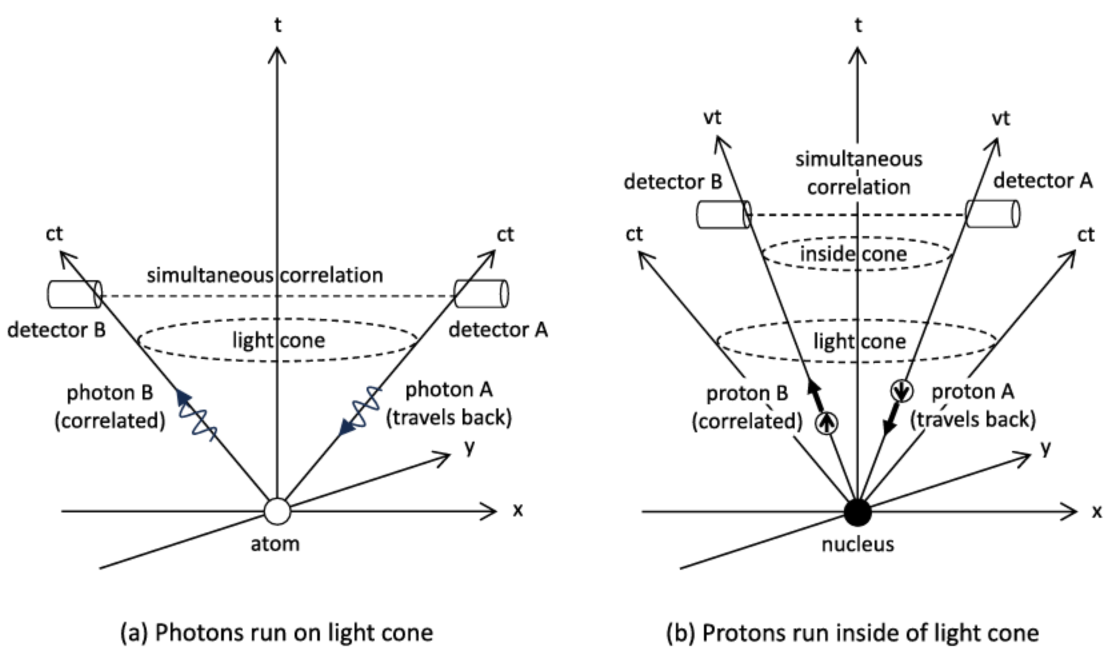

Figure 17: Relativistic causality of simultaneous correlation

As explained in Figure 16(a)(b) in this study, the photon detected by detector A has a fixed energy, so time reversal occurs, and the state goes back to the position and time of the atom that emitted the photon. At this point, the quantum entanglement in the superposition state is fixed as a single quantum entanglement, and the atom emits another entangled photon in opposite direction. If each detector is equidistant from the atom, the time at which the photon arrives at detector B in the opposite direction coincides with the time at which the photon arrived at detector A. The states of these entangled photon pairs are correlated. The state of one of these photons cannot be determined unless the state of the other photon is observed and determined. This simultaneous correlation appears to violate relativistic causality as a faster-than-light signaling event. However, according to this study, the observed photon first travels back in time and correlates with another photon. This correlated photon then arrives in the present when the observation was made, forming a correlated state with the other photon in the present. In this way, causality is connected from the present to the past and from the past to the present, so there is no violation of relativistic causality.

This study deals with Aspect's 1982 experiment using photons, so the detected photon travels back in time along the light cone as shown in Figure 17(a), while the entangled pair travels forward in time along the light cone in the opposite spatial direction. In the case of quanta such as protons [11], which travel slower than the speed of light, they also travel back in time along the inside of the light cone as shown in Figure 17(b), while the entangled pair travels back in time along the inside of the light cone in the opposite spatial direction.

Since the observed quantum moves inside or on the light cone, this theory is valid within the framework required by the theory of special relativity. Furthermore, their temporal behavior follows the unitary transformation and the antiunitary transformation with respect to time obtained from the fundamental equations of quantum mechanics. Therefore, this theory is completely in line with conventional quantum mechanics.

3.4 Applicability to General Quanta

The equation-level treatment of general quantum physics, including the Dirac equation and the Klein-Gordon equation, is as follows:

The Dirac equation below has a first-order time derivative, just like the Schrödinger equation:

$$i\hbar\frac{\partial}{\partial t}|\psi(\mathbf{x},t)\rangle = (c\boldsymbol{\alpha}\cdot\hat{\mathbf{p}} + \beta mc^2)|\psi(\mathbf{x},t)\rangle. \tag{70}$$

Applying the time-reversal transformation (3) and taking the complex conjugate of the whole, it becomes same form of the original Dirac equation as follows:

$$i\hbar\frac{\partial}{\partial t}\langle\psi(\mathbf{x},t)| = \langle\psi(\mathbf{x},t)|(c\boldsymbol{\alpha}\cdot\hat{\mathbf{p}} + \beta mc^2). \tag{71}$$

Therefore, the time-reversed solution evolves over time as a bra vector, similar to the discussion of the Schrödinger equation.

On the other hands, the Klein-Gordon equation has a second-order time derivative as follows:

$$-\frac{1}{c^2}\frac{\partial^2}{\partial t^2}|\psi(\mathbf{x},t)\rangle = \left(-\nabla^2 + \frac{m^2c^2}{\hbar^2}\right)|\psi(\mathbf{x},t)\rangle. \tag{72}$$

Applying the time-reversal transformation as in (3), the form of the equation does not change. Also, since there is no imaginary unit in each term, even if taking the complex conjugate of the whole, the form of the equation does not change, and we can see that the time-reversal solution evolves over time as a bra vector in the same equation.

$$-\frac{1}{c^2}\frac{\partial^2}{\partial t^2}\langle\psi(\mathbf{x},t)| = \langle\psi(\mathbf{x},t)|\left(-\nabla^2 + \frac{m^2c^2}{\hbar^2}\right). \tag{73}$$

In this way, it can be seen that the time reversal theory in this study also holds true in relativistic quantum mechanics.

4. Interpretation of the Randomization in Quantum Measurement Outcomes [44]

Quantum mechanics has fundamentally transformed the established Newtonian worldview. Specifically, it has revealed that measurement probabilistically determines quantum mechanical states and that this process is inherently nondeterministic. Thus, quantum mechanics rejects naive realism, which assumes that the state of a physical system is defined prior to measurement. In parallel, it also dismisses a deterministic worldview wherein the future state of a system is entirely determined by its temporal evolution. Instead, it provides probabilistic predictions of state determination through measurement and specifies the corresponding expected values of physical quantities. Moreover, individual measurement outcomes are considered to be random in principle. Notably, the success of quantum mechanics has substantiated these perceptions and profoundly influenced both philosophy and ontology. Accordingly, these statements constitute the foundational postulates of quantum mechanics.

As a counterargument, the hidden variable theory posits that quantum systems evolve according to undiscovered hidden variables [26]. Meanwhile, observations of entangled quantum systems have confirmed violations of Bell's inequality, indicating that hidden variables predetermining the state of a system prior to observation do not exist [46]. However, this finding does not necessarily imply that measurements determine the physical system in a nondeterministic manner. Even if hidden variables determining the state of a system prior to measurement are absent, those determining the state of the system during measurement may exist. In other words, hidden variables of the measuring device may deterministically govern outcomes during the measurement process. Notably, a quantum system exhibiting entanglement is interpreted as a state of unity, and observing one of its quantum components instantaneously alters the state of the other. This interpretation contradicts conventional local realism and is also inconsistent with the conclusions of special relativity [45].

As explained in Chapter 3, assuming a time-reversal vector created by observation allows the instantaneous correlations of an entangled quantum system to be interpreted as the result of proximity interactions due to negative and positive time evolution [14].

Meanwhile, the study of Chapter 1 hypothesized that observation determines the magnitude of the energy dispersion of each quantum state and that the resulting time uncertainty generates a time-reversal vector. Within this framework, the state that extends furthest into the past, that is, the state with the smallest energy dispersion, is considered the observed result. Accordingly, this interpretation asserts that measurement results are not determined randomly. However, the process by which observation determines the magnitude of the energy dispersion of each quantum state remains unclear.

To address this limitation, this study clarifies the above process by applying coherent measurement and measurement-based control [47] to general measurements. The findings reveal that phase differences among multiple states within the measurement system determine the magnitude of the energy dispersion of a quantum state and that these phase differences influence the energy dispersion of the quantum state at the time of measurement. In practice, realizing phase control during general measurements is difficult, leading to probabilistic outcomes; however, the process remains deterministic in principle.

4.1 Randomization of Energy Dispersion during Measurement

As indicated above, the magnitude of the energy dispersion of each state at the time of measurement determines the measurement outcomes randomly. However, existing measurement frameworks have not explained why the magnitude of the energy dispersion in each state is determined randomly. Previous quantum mechanics analyses also have not explained this mechanism, and the prevailing view is that measurement determines the state randomly in principle. Overall, this perspective has contributed to a departure from the Newtonian worldview, according to which the world evolves deterministically over time. Below, we demonstrate that phase differences among the states of the measuring device deterministically yield the magnitude of the energy dispersion in each measurement state. This indicates that uncontrollable phase differences among the states of the measuring device determine measurement results randomly.

Quantum measurement theory indicates that coherently controlling the quantum state of a measuring device alters its energy dispersion [47]. This topic falls within the framework of coherent measurement and measurement-based control. The primary considerations are as follows: When the measuring device is treated as a quantum state rather than a classical pointer and its phase is controllable, the time evolution of the energy dispersion of the measured system changes. In other words, measurement is treated not merely as decoherence but as a quantum interaction involving interference. This indicates that even when phase control is not achievable, the time evolution of the energy dispersion of the system under measurement undergoes uncontrollable yet deterministic changes. Below, we present a mathematical model based on quantum measurement theory [47].

When measuring the energy operator $\widehat{H}$, the energy eigenbase of the system becomes

$$\widehat{H}|E_i\rangle = E_i|E_i\rangle. \tag{74}$$

Here, the initial state is defined as

$$|\psi\rangle = \sum_i c_i\,|E_i\rangle. \tag{75}$$

Meanwhile, the state of the entire system $|\Psi\rangle$, including the pointer state $|\phi_i\rangle$ of the measuring device, is defined as

$$|\Psi\rangle = \sum_i c_i\,|E_i\rangle \otimes |\phi_i\rangle. \tag{76}$$

Further, the density matrix $\hat{\rho}_{SM}$ the entire system is defined as

$$\begin{aligned} \hat{\rho}_{SM} &= |\Psi\rangle\langle\Psi| \\ &= \sum_{j,i} c_i\,c_j^*|E_i\rangle\langle E_j| \otimes |\phi_i\rangle\langle\phi_j| \end{aligned} \tag{77}$$

Subsequently, a partial trace over the measuring device using the complete orthogonal basis $\{|k\rangle\}$ of the measuring device yields

$$\begin{aligned} \hat{\rho}_S &= \mathrm{Tr}_M(\hat{\rho}_{SM}) \\ &= \sum_k \langle k|\,\hat{\rho}_{SM}|k\rangle \\ &= \sum_k \sum_{j,i} c_i\,c_j^*\langle k|\big(|E_i\rangle\langle E_j| \otimes |\phi_i\rangle\langle\phi_j|\big)|k\rangle \\ &= \sum_{j,i} c_i\,c_j^*\,(|E_i\rangle\langle E_j| \sum_k \langle k|\,\phi_i\rangle\langle\phi_j|k\rangle). \end{aligned} \tag{78}$$

Here, the derivation uses the tensor product property $\langle k|(A \otimes B)|k\rangle = A \cdot \langle k|B|k\rangle$. Substituting a part of this equation yields

$$\begin{aligned} \sum_k \langle k|\,\phi_i\rangle\langle\phi_j|k\rangle &= \sum_k \langle\phi_j|\,k\rangle\langle k|\phi_i\rangle \\ &= \langle\phi_j|\phi_i\rangle \\ &= \Gamma_{ji}. \end{aligned} \tag{79}$$

The above formula is

$$\hat{\rho}_S = c_i c_j^* \Gamma_{ji}|E_i\rangle\langle E_j|. \tag{80}$$

Here, Γ_{ji} represents the overlap between different pointer states in the off-diagonal terms of the measuring device, and $c_i c_j^*$ represents phase information. The expectation value of the energy is calculated using the density matrix as

$$\begin{aligned} \langle\hat{H}\rangle &= \mathrm{Tr}\big(\hat{\rho}_S\hat{H}\big) \\ &= \sum_i |c_i|^2\,E_i. \end{aligned} \tag{81}$$

Further, the expectation value of the square of energy is

$$\begin{aligned} \langle \hat{H}^2 \rangle &= \mathrm{Tr}\left(\hat{\rho}_S \hat{H}^2\right) \\ &= \sum_i |c_i|^2 E_i{}^2 + \sum_{j \neq i} c_i c_j^* \Gamma_{ji} E_j E_i. \end{aligned} \tag{82}$$

Therefore, the expectation value of the squared energy dispersion is

$$\langle \Delta H \rangle^2 = \sum_i |c_i|^2 E_i{}^2 - \left(\sum_i |c_i|^2 E_i\right)^2 + \sum_{j \neq i} c_i c_j^* \Gamma_{ji} E_j E_i. \tag{83}$$

In the von Neumann measurement framework, the interaction Hamiltonian $\hat{H}_{int}$ between system S and measuring device M is expressed as [1].

$$\hat{H}_{int} = g\hat{H} \otimes \hat{P}. \tag{84}$$

The initial state of the measuring device is $|\phi_0\rangle$, while its overall state after measurement is defined as

$$|\Psi\rangle = \sum_i c_i\, |E_i\rangle |\phi_i\rangle. \tag{85}$$

Under typical conditions, the off-diagonal term Γ_{ji}, which represents the state of the measuring device after measurement, approaches zero due to decoherence, and interference vanishes:

$$\Gamma_{ji} = \langle \phi_j | \phi_i \rangle \approx 0. \tag{86}$$

Next, we consider the case in which the measuring device is in a phased superposition state, as given by

$$|\phi_0\rangle = \frac{1}{\sqrt{2}}\left(|p_1\rangle + e^{i\theta}|p_2\rangle\right). \tag{87}$$

The unitary time evolution operator is defined as

$$\hat{U} = e^{-ig\hat{H}\otimes\hat{P}}. \tag{88}$$

Applying this to (85) yields

$$\begin{aligned} |\Psi\rangle &= \sum_i c_i\, |E_i\rangle \hat{U} |\phi_0\rangle \\ &= \sum_i c_i\, |E_i\rangle e^{-ig\hat{H}\otimes\hat{P}} \frac{1}{\sqrt{2}}\left(|p_1\rangle + e^{i\theta}|p_2\rangle\right) \\ &= \sum_i c_i\, |E_i\rangle \frac{1}{\sqrt{2}}\left(e^{-igE_i p_1}|p_1\rangle + e^{i\theta} e^{-igE_i p_2}|p_2\rangle\right). \end{aligned} \tag{89}$$

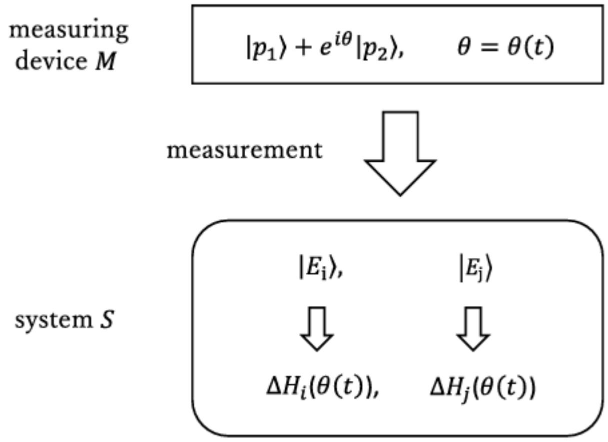

Figure 18:Measurement with phased superposition state device

To eliminate the degrees of freedom of the measuring device, a partial trace over the measuring device M is taken, as shown in (80):

$$\hat{\rho}_S = \mathrm{Tr}_M(|\Psi\rangle\langle\Psi|) = \sum_{j,i} c_i\, c_j^* \Gamma_{ji} |E_i\rangle\langle E_j|. \tag{90}$$

In this case,

$$\Gamma_{ji} = \frac{1}{2}\left(e^{-ig(E_i-E_j)p_1} + e^{-ig(E_i-E_j)p_2} e^{i\theta}\right). \tag{91}$$

In quantum controlled measuring devices,

$$\Gamma_{ji} \neq 0. \tag{92}$$

Therefore, the energy dispersion of each state in (83) is phase-dependent, as indicated in (91). In contrast, ordinary measuring devices are strongly coupled to the environment, and decoherence leads to

$$\Gamma_{ji} \to 0. \tag{93}$$

This occurs when the measurement reaches its final stage. This study examines the state of the system when the measurements described in Chapter 1 are performed, prior to definitive state determination. Specifically, at this stage, each state is not yet strongly coupled to the environment, and $\Gamma_{ji} \neq 0$. Accordingly, even when a conventional measuring device is used, the immediate post-measurement stage, in which states remain undetermined and coexist, exhibits inter-state interference components as described in (91).

In this context, according to (83), the energy dispersion of each state is defined as

$$\Delta H_i = \sqrt{|c_i|^2 {E_i}^2 - (|c_i|^2 E_i)^2 + \sum_{j(\neq i)} c_i\, c_j^* \Gamma_{ji} E_j E_i}. \tag{94}$$

Notably, the phase θ is added to the interference factor Γ_{ji} between states, as indicated in (91). Since (91) is a complex number, the observable (94) is also a complex number. This is because this system is an open quantum system that is in the process of interacting with its environment. Thus, (94) can be expressed as

$$\Delta H_i = \mathrm{Re}(\Delta H_i) - i\mathrm{Im}(\Delta H_i). \tag{95}$$

The time evolution of the state is then given by

$$\psi_i(t) \sim e^{-i\frac{\mathrm{Re}(\Delta H_i)}{\hbar}t} e^{-\frac{\mathrm{Im}(\Delta H_i)}{\hbar}t}. \tag{96}$$

The imaginary part in the above relation causes exponential decay in amplitude. Thus, it represents the rate of decoherence rather than the observed value. However, the real part can be obtained at the final stage of measurement.

In the intermediate stage of measurement, the energy dispersion of each state depends on phase differences between the superposition states of the measuring device, even when using ordinary measuring devices that are not quantum controlled. This constitutes an uncontrollable yet deterministic effect of standard measurements.

As described in Chapter 1, each state undergoes time dispersion in a manner inversely proportional to its energy dispersion and ultimately settles into the state that has reached furthest in the past. Consequently, the phase of the superposition state of the measuring device deterministically determines the final state. Since phases in a typical measurement system are not controlled, phase differences fluctuate, resulting in $\theta = \theta(t)$. The above scenario is depicted in Figure 18. Accordingly, the measured state depends on the timing of the measurement. This introduces randomness into the measurement results, although the process remains fundamentally deterministic. This therefore challenges the non-deterministic interpretation of measurement results in conventional quantum mechanics.

4.2 Experimental Verification

We expect that a quantum-controlled measuring device may confirm that energy dispersion depends on phase differences between the superposition states of the measuring device. Furthermore, measuring phase-dependent variations in the energies of coexisting states using weak measurements would further validate this study. Specifically, Ramsey interferometry, which measures the phase of qubits, may be used. In applying this approach to the present study, a measurement pointer will be required instead of a qubit. The complex weak value corresponds to the amplitude and phase of the interference. Previous studies have directly measured the complex weak value in neutron interference [49].

5. Discussion

5.1 Compatibility with Theorems Refuting the Hidden Variable Theory

The hidden variable theory asserts that a physical system simultaneously possesses definite values for all physical quantities through underlying hidden variables. However, two representative theorems demonstrate the impracticality of such a theory. These include von Neumann's no-go theorem and the Kochen-Specker theorem [1,50]. Specifically, von Neumann's no-go theorem states that a state with zero dispersion for all physical quantities does not exist. Similarly, the Kochen-Specker theorem states that a contradiction arises if one assigns "1" to one vector in an orthogonal basis and "0" to the others across all such bases.

This study assumes that the physical system before measurement remains in an undetermined state and does not simultaneously possess definite values for all physical quantities. Therefore, the present analysis does not require hidden variables that determine the state of the physical system before measurement. Consequently, von Neumann's no-go theorem applies to this study because it assumes states with nonzero dispersion. Similarly, the Kochen-Specker theorem also applies because this study does not attempt to assign "1" to one vector in an orthogonal basis and "0" to the others across all such bases.

5.2 Reconciliation with Einstein's Dissent

During the early development of quantum mechanics, Einstein and others raised concerns regarding its rejection of local reality and deterministic behavior during measurements [46]. In this context, local reality comprises two components:
(a) [Reality]: Physical existence refers to a state determined prior to measurement.
(b) [Locality]: When systems interact at a distance, the interaction requires sufficient time to propagate at the speed of light.

However, experiments conducted by Aspect et al.[13] verified violations of Bell's inequality [45] in entangled quantum states, thereby disproving these assumptions. Moreover, violations of Bell's inequality exclude the possibility that a hidden variable predetermines the state. As the study of Chapter 1, it maintains that quantum mechanical states in superposition are not uniquely determined prior to observation [4], thereby rejecting the existence of (a). However, the study of Chapter 3 offered an interpretation of the mechanism underlying instantaneous correlations in quantum entanglement [14]. Specifically, this correlation propagates retrogradely via time-reversed waves and can therefore be interpreted as a local interaction. Consequently, quantum mechanically determined reality does not violate locality because it transmits effects to distant quanta along both positive and negative temporal directions, which ultimately cancel.

The study of Chapter 4 also explains the following concept.
(c) [Determinism]: Measurement results are determined deterministically.
Specifically, this study shows that even seemingly random measurement results depend on the uncontrollable phase of the measurement system at the time of measurement, resulting in variability. Therefore, this study supports determinism in measurement. The conclusions of this series of studies are as follows:
(a) "Reality" is denied, consistent with the conventional interpretation of quantum mechanics.
(b) "Locality" is affirmed, in contrast to the conventional interpretation of quantum mechanics.
(c) "Determinism" is affirmed, in contrast to the conventional interpretation of quantum mechanics.

Regarding "reality" in (a), quanta are considered to exist as wave phenomena in a vacuum, and their manifestation as particles emerges upon collapse during observation [31]. In other words, if the state prior to measurement is regarded as the true reality, then its reality is affirmed. Accordingly, these results reconcile Einstein's intuitions with quantum mechanics without altering its formal structure. Overall, the aim of the author's studies was to eliminate ontological ambiguities in quantum mechanics and facilitate intuitive interpretation. These studies do not alter the fundamental structure of quantum mechanics. Therefore, they do not affect the established successes of quantum mechanics.

6. Conclusion

This study interprets quantum-mechanical observation as involving quanta that propagate backward in time. Time retrogression is regarded as a property permitted by the energy–time uncertainty relation, according to which a system with constant energy may exhibit fluctuating time evolution. Specifically, time reversal is described by an antiunitary transformation wherein the state vector becomes the complex conjugate of the original state vector. If the original state vector is a ket vector, its complex conjugate is a bra vector.

When a time-dependent bra vector and a ket vector interact along the time axis, they establish a time-invariant bra-ket state. The establishment of this bra–ket state explains observation-induced quantum state contraction. According to the energy–time uncertainty relation, the state with the lowest observation-induced energy dispersion exhibits the largest time dispersion. Accordingly, this state can transmit a time-reversed bra vector to the farthest point in the past, thereby forming a bra–ket state and eliminating other states.

Time fluctuation also occurs in the future; once the “present” exceeds the fluctuation time, only the time-invariant state remains. This process results in observation-induced quantum state contraction. This theory is consistent with the widely accepted interpretation of the energy–time uncertainty relation involving the time scale of state establishment.

This study also examines the mechanism underlying the spatial contraction of a wave packet upon observation. In the above configuration, spatial contraction is yet to occur. However, the dot product terminates time evolution, resulting in a stationary state. Within quantum field theory, the wave functions constituting the wave packet arise from vacuum energy fluctuations, and pressure associated with vacuum energy originates from these fluctuations. However, the dot product eliminates these fluctuations in the bra–ket state. Consequently, the bra–ket state domain experiences external compressive pressure from vacuum energy. This external pressure spatially contracts the wave packet. Thus, this framework is proposed as the mechanism underlying both state selection and spatial contraction of the wave packet upon observation.

This study interpreted EPR correlation as a long-range correlation without transmission time . In Aspect’s experimental system, a detector determines the polarization state of a photon, its bra vector travels backward in time and determines the polarization state on the other side of the photon, and the resulting correlation remains consistent with special relativity. This theory is useful not only for interpreting Aspect’s experiments but also for directly describing state determination through quantum-mechanical observations.

The study also explains the origin of observational randomness through randomness in the magnitude of energy dispersion during observation. Specifically, during coherent measurements, phase differences between the states of the measuring device affect the energy dispersion of measurement results. Even during standard measurements, however, phase differences persist in each measuring-device state until decoherence eliminates them. This persistence accounts for randomness in each state’s energy dispersion at the moment of measurement. Nevertheless, this randomness arises from an underlying deterministic process. Overall, this result eliminates inherent indeterminism in quantum-mechanical phenomena and indicates that quantum systems evolve deterministically over time.

7. Declarations

7.1 Ethical Approval

Not applicable. This study did not involve human participants or animal subjects.

7.2 Competing Interests

The author declares that there are no competing interests, or other financial or non-financial interests that could be perceived to have influenced the results or discussion presented in this paper.

7.3 Authors' Contributions

Yoshiya Higuchi wrote the manuscript and prepared all figures.

7.4 Funding

This research did not receive funding from any public, commercial, or not-for-profit funding agency. No grant numbers are associated with this study.

7.5 Availability of Data and Materials

All data generated or analyzed during this study are included in this published article.

References

1. von Neumann J (1932) *Die Mathematische Grundlagen der Quantenmechanik*. Springer, Verlag.
2. Gao S (2017) *The meaning of the wave function, in search of the ontology of quantum mechanics*, Cambridge University Press.
3. Gao S, et al. (2018) C*ollapse of the wave function, models, ontology, origin, and implications,* Cambridge University Press.
4. Higuchi Y (2025) Interpretation of quantum state contraction due to time-retrograde waves in observation process, *Int. J. Quantum Found* **11**: 664-687.
5. De Broglie L (1934) Sur la nature de photon, *Comptes Rendus* 198.
6. Costa de Beauregard O (1976) Time Symmetry and Interpretation of Quantum Mechanics *Found. Phys* **6**: 5.
7. Cramer JG (2015) The Transactional Interpretation of Quantum Mechanics and Quantum Nonlocality. arXiv:1503.00039v1 [quant-ph] **28**.
8. Aharonov Y, Vaidman L (2017) The Two-State Vector Formalism: An Updated Review. arXiv:0105101v2 [quant-ph] **10**.
9. Pegg D (1982) Time symmetric electrodynamics and the Kocher-Commins experiment. *Eur. J. Phys* **3**: 44.
10. Wheeler J, Feynmann R (1945) Interaction with the absorber as the mechanism of radiation. Rev. Mod. Phys. 17: 157.
11. Sakai H (2003) Spin Entanglement Measurement of Two Protons, J. Phys. Soc. Jap 72: C193-C195.
12. Cramer JG (2016) *The Quantum Handshake*, Springer 63-64.
13. Aspect A, Dalibard J, Roger G (1982) Experimental test of Bell's inequalities using varying analyzers. *Phys. Rev. Lett* **49**: 1804.
14. Higuchi Y (2025) Interpretation of simultaneous correlation in quantum entanglement with retrocausality. *Int. J. Quantum Found* **11**: 596-610.
15. Pauli W (1933) *Die allgemeinen Prinzipien der Wellenmechanik*, *Handbuch der Physik*, Bd. XXIV, Teil 1.

16. Busch P (2022) The time-energy uncertainty relation. In Time in quantum mechanics; Muga, J.G.; Mayato, R.S.; Egusquiza, I.L., Eds.; Springer: Berlin, Lecture Notes in Physics **72**.
17. Mandelstam LI, Tamm IY (1945) The uncertainty relation between energy and time in nonrelativistic quantum mechanics. *J. Phys* **9**: 249-254.
18. Arai A (2007) Spectrum of time operators, *Lett. Math. Phys* **80**: 211-221.
19. Sakurai JJ, Napolitano JJ (2010) *Modern Quantum Mechanics*, 2nd Edition. Harlow, Person.
20. Tonomura A, et al. (1989) Demonstration of single-electron buildup of interference pattern. *Am. J. Phys* **57**: 117.
21. Guryanova YG, et al. (2019) Ideal Projective Measurements Have Infinite Resource Costs, arXiv:1805118991v3 [quant-ph] **18**.
22. Aharonov Y, et al. (1998) How the result of a measurement of the spin-1/2 particle can turn out to be 100, *Phys. Rev. Lett*. **60**: 1351.
23. Gourgy H, et al. (2016) Quantum dynamics of simultaneously measured non-commuting observables, *Nature* **538**: 491-494.
24. Ficheux Q, et al. (2018) Dynamics of a qubit while simultaneously monitoring its relaxation and dephasing, *Nature communications* **9**: 1926.
25. Scully MO, et al. (1991) Quantum optical tests of complementarity, *Nature* **351**.
26. Wheeler JA, Zurek WH (2014) *Quantum Theory and Measurement*, Princeton Legacy Library.
27. Dressel J, et al. (2017) Arrow of time for continuous quantum measurement, *Phys. Rev. Lett* **119**: 220507.
28. Manikandan SK, Jordan AN (2018) Time reversal symmetry of generalized quantum measurements with past and future boudary conditions, arXiv:1801.04364v2 [quant-ph].
29. Rovelli C (1993) Statistical mechanics of gravity and the thermodynamical origin of time, 4, 020309 (2023) *Class. Quamtum Grav* **10**: 1549-1566.
30. Connes A, Rovell C (1994) Von Neumann algebra automorphisms and time-thermodymanics relation in general covariant quantum theories, arXiv: gr-qc/9406019v1.
31. Higuchi Y (2026) QFT-based interpretation of the spatial contraction of a wave packet upon observation, *Int. J. Quantum Found* **12**: 248-261.
32. Peracaula JS, Mareno-Pulido C (2024) Vacuum energy and cosmological constant in QFT in curved spacetime. arXiv: 2411.06582v1 [hep-th] **10**.
33. Diósi L (2013) Gravity-related wave function collapse: mass density resolution, arXiv:1302.5365v1[quant-ph] **21**.
34. Corichi A, et al. (2022) On the Schrödinger representation for a scalar field on curved spacetime, arXiv: gr -qc/ 0207088v1 **24**.
35. Prasad R, et al. (2025) Reconstruction of quantum states by applying an analytical optimization model*,* arXiv: 2501.07404v1 **13**.
36. Tong D (2007) Q*uantum field theory, University of Cambridge Part III Mathematical Tripos*, Michaelmas Term.
37. Lamoreaux SK (1997) Demonstration of the Casimir force in the 0.6 to 6μm range, *Phys. Rev. Lett* **78**: 5.
38. Casimir HBG (1948) On the attraction between two perfectly conducting plates, Proc. Koninkl. *Ned. Akad. Wetenschap* **51**: 793.
39. Zee A. *Quantum field theory in a Nutshell 2nd Edition*, Princeton University Press.
40. Hodgson D, Southall J, Puedy R, Beige A. Local photons; *Front. Photn* **3**: 978855.
41. Hawton M (2021) Photon quantum mechanics in real Hilbert space, arXiv:2107.03262v3 [quantph] **4**.

42. Southall J, Hodgson D, Puedy R, Beige A (2021) Locally-acting mirror Hamiltonians; *J. Mod. Opt*. **68**: 647.
43. Recommendation 2 (2007) On the value and uncertainty of unstabilised He-Ne lasers 96th CIPM (2007).
44. Higuchi Y (2026) Interpretation of the randomization in quantum measurement outcomes, *Int. J. Quantum Found* **12**: 854-866.
45. Bell JS (1964) On the Einstein Podolsky Rosen paradox. *Physics* **1**: 195-200.
46. Einstein A, Podolsky B, Rosen N (1935) Can quantum-mechanical description of physical reality be considered complete? *Phys. Rev* **47**: 777-780.
47. Wiseman HM, Milburn G J (2010) *Quantum Measurement and Control*, Cambridge University Press.
48. Dressel J, et al. (2014) Colloquium: Understanding quantum weak values: Basics and applications, arXiv, 1305.7154v2[quant-ph] **1**.
49. Sponar S, et al. (2015) Weak values obtained in matter-wave interferometry, *Phys. Rev. A* **92**: 062121.
50. Kochen S, Specker E (1975) The problem of hidden variables in quantum mechanics, *J. Math*. Mech **17**: 59-87.